Amyotrophic Lateral Sclerosis Modifiers in *Drosophila* Reveal the Phospholipase D Pathway as a Potential Therapeutic Target

Mark W. Kankel,* Anindya Sen,*,[1] Lei Lu,[†] Marina Theodorou,[‡] Douglas N. Dimlich,[‡] Alexander McCampbell,* Christopher E. Henderson,* Neil A. Shneider,[†] and Spyros Artavanis-Tsakonas[‡,2]

*Neuromuscular and Movement Disorders Research Unit, Biogen, Cambridge, Massachusetts 02142, [†]Department of Neurology, Center for Motor Neuron Biology and Disease, Columbia University, New York 10032, and [‡]Department of Cell Biology, Harvard Medical School, Boston, Massachusetts 02115

ORCID ID: 0000-0001-9112-1518 (S.A.-T.)

ABSTRACT Amyotrophic lateral sclerosis (ALS), commonly known as Lou Gehrig's disease, is a devastating neurodegenerative disorder lacking effective treatments. ALS pathology is linked to mutations in >20 different genes indicating a complex underlying genetic architecture that is effectively unknown. Here, in an attempt to identify genes and pathways for potential therapeutic intervention and explore the genetic circuitry underlying *Drosophila* models of ALS, we carry out two independent genome-wide screens for modifiers of degenerative phenotypes associated with the expression of transgenic constructs carrying familial ALS-causing alleles of FUS ($hFUS^{R521C}$) and TDP-43 ($hTDP\text{-}43^{M337V}$). We uncover a complex array of genes affecting either or both of the two strains, and investigate their activities in additional ALS models. Our studies indicate the pathway that governs phospholipase D activity as a major modifier of ALS-related phenotypes, a notion supported by data we generated in mice and others collected in humans.

KEYWORDS Amyotrophic lateral sclerosis (ALS); TDP43; FUS; C9ORF72; phospholipase D (PLD)

AMYOTROPHIC lateral sclerosis (ALS), commonly known as Lou Gehrig's disease, is a devastating neurodegenerative disorder that selectively involves motor neurons (MNs) in the brain and spinal cord, resulting in progressive muscle weakness and atrophy (Rowland 2001). Nearly all patients with ALS eventually succumb to respiratory failure 3–5 years after disease onset (Brown and Al-Chalabi 2017). The ALS association (http://www.alsa.org/) estimates that the incidence of ALS is ~2 per 100,000 people. Because of disease severity, the rapid course of the disease, and lack of effective treatments, there is a great unmet need to develop novel therapies (Moujalled and White 2016; Abe *et al.* 2017; Hardiman and van den Berg 2017). ALS pathology has been linked to mutations in >20 different genes indicating a complex underlying genetic architecture (Gros-Louis *et al.* 2006; Maruyama *et al.* 2010; Turner *et al.* 2013). Nevertheless, mutations identified via genome-wide association studies account for only 5–10% of cases (familial ALS; fALS) (Rothstein 2009; Byrne *et al.* 2011; Bunton-Stasyshyn *et al.* 2015). The remaining cases are defined as sporadic ALS (sALS) and occur in individuals who lack familial inheritance of known fALS genetic variants. fALS variants have been identified in some individuals within sALS populations (Gibson *et al.* 2017), reflecting the complex genetic circuitry and the potential occurrence of *de novo* mutations associated with ALS.

Two dominant mutations in *Fused in Sarcoma* (*FUS*) and *Transactive Response DNA binding protein 43 kD* (*TARDBP*; encoding the TDP-43 protein), have been shown to cause fALS, and also some rare cases of frontotemporal lobar degeneration (Mackenzie *et al.* 2010). Both genes encode RNA-binding proteins (RBPs) as, indeed, several ALS-causal genes have been implicated in RNA metabolism, suggesting that this cellular function is closely associated with the disorder (Ito *et al.* 2017; Ghasemi and Brown 2018). Along with *FUS*

doi: https://doi.org/10.1534/genetics.119.302985
Manuscript received December 13, 2019; accepted for publication April 19, 2020; published Early Online April 28, 2020.
Available freely online through the author-supported open access option.
Supplemental material available at figshare: https://doi.org/10.25386/genetics.12202580.
[1]Present address: Prevail Therapeutics, New York, NY, 10016.
[2]Corresponding author: Department of Cell Biology, LHRRB-301C, Harvard Medical School, 250 Longwood Ave., Boston, MA 02115. E-mail: artavanis@hms.harvard.edu

and *TARDBP* (*TDP-43*), *Chromosome 9 open reading frame 72* (*C9orf72*) and *Superoxide dismutase 1* (*SOD1*) define the most prevalent fALS genes (Lagier-Tourenne *et al.* 2010; Ling *et al.* 2013; Turner *et al.* 2013; Renton *et al.* 2014). Both FUS and TDP-43 proteins are ubiquitously expressed, predominantly localized to the nucleus where they are implicated in various aspects of RNA metabolism (Crozat *et al.* 1993; Prasad *et al.* 1994; Buratti and Baralle 2001; Iko *et al.* 2004; Andersson *et al.* 2008; Ayala *et al.* 2008; Winton *et al.* 2008; Tan and Manley 2009; Kato *et al.* 2012; King *et al.* 2012; Deng *et al.* 2014). TDP-43- and FUS-associated pathologies are characterized by formation of intracellular protein aggregates in brain and spinal cord neurons and glia, a phenomenon shared by many neurodegenerative diseases (Arai *et al.* 2006; Neumann *et al.* 2006; Kwiatkowski *et al.* 2009b; Vance *et al.* 2009; Tateishi *et al.* 2010).

The pioneering work of the Bonini laboratory has demonstrated the utility of *Drosophila* as an experimental system to investigate neurodegenerative diseases, and ALS in particular (McGurk *et al.* 2015; Goodman and Bonini 2020). To better understand the involvement of TDP-43 and FUS in ALS and to probe the genetic circuitry that underlies ALS-related pathology, we took advantage of the genetic tools offered by *Drosophila* to systematically identify modifiers of TDP-43- and FUS-related phenotypes. We assume that the identification of genes capable of modifying ALS-related phenotypes in animal models may point to promising therapeutic targets and potentially novel pathways involved in disease. The *Drosophila* genome contains orthologs of most of the known ALS-causal genes, including *TAR DNA-binding protein-43 homology* (*TBPH* aka *dTDP-43*) and *cabeza* (*caz* aka *dFUS*), orthologs of *TDP-43* and *FUS*, respectively. The phenotypes associated with mutations in these two genes, or with ectopic expression of human variants, manifest in several tissues known to be affected in patients with ALS.

In *Drosophila*, loss of *dTDP-43* is semilethal (Feiguin *et al.* 2009; Wang *et al.* 2011), causing reduced larval motility and disruptions in neuromuscular junction (NMJ) morphology (Feiguin *et al.* 2009; Wang *et al.* 2011). Neuronal overexpression of wild-type human TDP-43 (hTDP-43) causes a decrease in NMJ bouton and branch number associated with protein aggregates (Li *et al.* 2010), indicating that loss or gain of TDP-43 function affects NMJ morphology. Other studies confirmed that overexpression of wild-type or mutant hTDP-43 in *Drosophila* or mice leads to locomotor defects (Wegorzewska *et al.* 2009; Li *et al.* 2010; Ritson *et al.* 2010; Voigt *et al.* 2010; Estes *et al.* 2011; Lin *et al.* 2011; Miguel *et al.* 2011). Expression of any of several hTDP-43 transgenic constructs carrying wild-type and disease-associated alleles in the developing *Drosophila* eye cause roughness, loss of pigmentation and neuronal degeneration (Li *et al.* 2010; Ritson *et al.* 2010; Voigt *et al.* 2010; Estes *et al.* 2011; Lin *et al.* 2011; Miguel *et al.* 2011).

Loss of dFUS causes reduced eclosion rates and life span, as well as locomotion defects (Wang *et al.* 2011; Xia *et al.* 2012), phenotypes that are rescued by neuronal expression of *Drosophila* or human FUS, reflecting a conserved function (Wang *et al.* 2011). Furthermore, expression of several fALS-linked missense alleles affecting the nuclear localization signal (NLS) in the *Drosophila* eye cause age- and dosage-dependent degeneration (Lanson *et al.* 2011). Ectopic expression of hFUS carrying ALS-causing variants (R518K or R521C) in *Drosophila* causes eye, brain, and MN degeneration (Daigle *et al.* 2013). Taken together, these observations reinforce the notion of functional conservation across species barriers, and our premise that *Drosophila* offers a suitable model to probe TDP-43 and FUS function.

Here, we explore the genetic circuitry that underlies *Drosophila* models of ALS by performing two independent genome-wide screens for enhancers and suppressors of the degenerative phenotypes associated with the expression of transgenic constructs carrying fALS-causing alleles of hFUS ($hFUS^{R521C}$) and hTDP-43 ($hTDP\text{-}43^{M337V}$). We uncover a complex array of genes that affect either, or both, of the two strains and corroborate these findings in secondary functional genetic assays using additional *Drosophila* ALS models we developed. Among the many modifying genes we identified, most of which have not been associated previously with ALS, these analyses also identify the pathway that governs phospholipase D (PLD) activity as a major modifier of ALS-related phenotypes. We further assessed the effect of PLD deletion in an *SOD1* mouse model of ALS and observed modest functional benefits. Thus, our studies afford novel insights into the genetic architecture that can modulate fALS-causing mutations, and importantly, point to novel genes and pathways that constitute potential targets for therapeutic intervention.

Materials and Methods

Drosophila stocks and culture

All *Drosophila* stocks were maintained on standard *Drosophila* medium at 25°C. The generation of the *GMR-hFUS*^{R521C} and *GMR-hTDP-43*^{M337V} screening strains has been previously described (Periz *et al.* 2015). We generated a *GMR-GAL4*, *UAS-c9orf72(G4C2)*$_{30}$*-EGFP* (*GMR-c9orf72*$_{30}$) recombinant line using the previously described GAL4 inducible *UAS-c9orf72(G4C2)*$_{30}$*-EGFP* transgenic strain (Xu *et al.* 2013). The full genotype of this strain is *w*; *GMR-GAL4*, *UAS-c9orf72* (1–8M)/*CyO*. All three dTDP-43 transgenic constructs were inserted into the pUASg.attB third chromosome site. We subsequently made a *GMR-Gal4/CyO*; *UAS-dTDP-43*^{mNLS}*/TM6B*, *Tb*, *Tub-GAL80* for analyzing dTDP-43 aggregates in third instar larval eye imaginal disc studies. In addition, we generated *OK371-GAL4*, *UAS-CD8-GFP/CyO*; *UAS-dTDP-43*^{N493D}*/TM6B*, *Tb*, *Tub-GAL80* strain for NMJ analyses. The *GMR-GAL4* and *TM6B*, *Tb Hu* chromosomes used to generate the screening stock were obtained from the Bloomington *Drosophila* Stock Center.

The following *Drosophila* strains were obtained from the Bloomington *Drosophila* Stock Center. GAL4-inducible RNA

interference (RNAi) knockdown, overexpression or expression of dominant negative versions of the following genes and associated Bloomington Stock Identifications (BSID): *ArfGAP3*^{RNAi}: BSID – 27183; *ArfGAP3*^{RNAi}: BSID – 31156; *Ask1*^{RNAi}: BSID – 32464; *Ask1*^{RNAi}: BSID – 35331; *futsch*^{EP1419}: BSID – 10571; *GLE1*^{RNAi}: BSID – 52888; *HDAC6* ^{RNAi}: BSID – 31053; *lilli*^{RNAi}: BSID – 26314; *Marf* ^{RNAi}: BSID – 31157; *Pld*^{RNAi}: BSID – 32839; *Rala*^{RNAi}: BSID – 34375; *Rala*$^{Dominant\ Negative}$: BSID – 32094; *Rgl*^{RNAi}: BSID – 28938; *SF2*^{RNAi}: BSID – 29522; and *SF2*^{RNAi}: BSID – 32367 .

The *UAS-dPld13* (Raghu *et al.* 2009) was a generous gift of Dr. Raghu Padinjat.

Generation of dTDP-43 transgenic constructs

CLUSTAL online software (Chenna 2003; Larkin *et al.* 2007) was used to align hTDP-43 and *Drosophila* TBPH (dTDP-43). Mouse and zebrafish TDP-43 orthologs were also used to improve the alignments (data not shown) (Supplemental Material, Figure S1). To construct the pUASg.attB-derived plasmids for the generation of the transgenic flies harboring the wild type or mutant forms of *dTDP43*, the wild-type genes were amplified from the pMK33-C-tbph plasmids (Guruharsha *et al.* 2011; Yu *et al.* 2011). The genes were initially cloned into the pDONR221 vector and followed by the final cloning into the pUASg.attB vector (Bischof *et al.* 2013) (a kind gift of Dr Konrad Basler). The mutations were subsequently introduced into the gene sequences using a QuickChange II Site Directed Mutagenesis Kit (Stratagene, La Jolla, CA).

Genetic modifier screens

Individual strains from the Exelixis Collection (Artavanis-Tsakonas 2004; Parks *et al.* 2004; Thibault *et al.* 2004) were tested for the ability to genetically modify the *GMR-GAL4*-induced *UAS-hFUS*^{R521C} and *UAS-hTDP-43*^{M337V} eye degeneration phenotypes by mating three to five males of the Exelixis strain to three females of the *GMR-GAL4/CyO*; *UAS-hFUS*^{R521C}*/TM6B*, *Tb*, *Tub-GAL80* and *GMR-GAL4*, *UAS-hTDP-43*^{M337V}*/CyO*, *Tub-GAL80* screening stocks. Fifteen days after being initiated, crosses were scored for alterations in the degenerative rough-eye phenotypes and/or restoration of pigmentation. Those inserts that improved the degenerative phenotypes were called suppressors (S), while those that made the phenotypes worse were deemed enhancers (E). The phenotypes were qualitatively scored from one to three; modifiers assigned a score of one are considered weak, a score of two is considered intermediate, and a score of three is considered strong. Those inserts scoring two or above were retested using a similar crossing scheme. Only those that displayed the same modification, independent of strength, were considered to be validated and therefore *bona fide* modifiers.

c9orf72 progressive model of neurodegeneration

Newly emerged *w*; *GMR-c9orf72*$_{30}$ animals exhibited weak roughness and slight disruptions to the ommatidial array with associated loss of pigmentation, suggestive of neurodegeneration (Figure 3), a phenotype that is dosage-sensitive as homozygous *GMR-c9orf72*$_{30}$ individuals result in a more severe phenotype (data not shown). To determine whether *GMR-c9orf72*$_{30}$ was indeed progressive, we aged a population of *GMR-c9orf72*$_{30}$ animals for 6 weeks and, at 3 different time points (weeks 1, 3, and 6), calculated the percentage of animals displaying black necrotic tissue, an indicator of *c9orf72(G4C2)*$_{30}$ neuronal degeneration (Zhang *et al.* 2015). Detection of a single black necrotic spot on a single eye within an individual was considered neurodegenerative and scored positive in this assay. Within the population of *GMR-c9orf72*$_{30}$/+ control animals, we observed an increase in the penetrance of the black necrotic tissue at weeks 1, 3, and 6 (Figure 3, E–H); this increase in the percentage of the degenerative phenotype was quantified and is displayed as a histogram in Figure 3I.

Drosophila gene assignments for the Exelixis Collection of transposon insertions

Data for *Drosophila* genes and Exelixis transposon insertion sites were obtained from FlyBase version 5.39, which was current as of August 2011 and is described elsewhere (Sen *et al.* 2013). The existing genomic sequence flanking all 15,500 inserts of the Exelixis Collection allowed for identification of affected genes (Sen *et al.* 2013). Using this analysis, we determined that the modifying insertions isolated by both screens combined correspond to a total of 758 total Exelixis strains, 205 strains unique to *GMR-hFUS*^{R521C}, 121 strains unique to *GMR-hTDP-43*^{M337V} and 432 strains recovered in both screens (Figure 2). We also identified 66 insertions (Table S1, column F, "Same modification") not included in the summary Venn diagrams in Figure 2 that acted as an enhancer for one screening strain and as a suppressor for the other. Modifying inserts for which no gene assignment could be determined failed to land within 1 kb of any gene or were in genomic regions that contain no annotated genes; several of which may have localized to regions near nonprotein coding RNA species that were not annotated at the time of the aforementioned analysis.

Mapping Drosophila genes to human orthologs

Version 7.1 (March 2018) of the DRSC Integrative Ortholog Prediction Tool (DIOPT) (http://www.flyrnai.org/cgi-bin/DRSC_orthologs.pl#) was used to determine the human orthologs, Human GeneID and the DIOPT ortholog score (Hu *et al.* 2011). The DIOPT ortholog score uses a 1–15 scale, where the higher the number, the better the orthology. It should be noted that for *Drosophila* genes for multiple human orthologs were determined, the ortholog with the highest DIOPT ortholog score is listed.

NMJ analyses

Third instar larvae were dissected in cold 1 × PBS and fixed at room temperature (RT) for 20 min in 4% paraformaldehyde. The samples were washed in 0.1% Triton X-100 in PBS (PTX) and incubated overnight at 4° with primary antibody. The

primary antibody was washed off with PTX at RT. The samples were incubated at RT with secondary antibody for 90 min. This was followed by a PTX wash, and the tissues were mounted in Vectashield mounting media with DAPI (Vector Laboratories). Bouton numbers were counted using a Zeiss 710 microscope, based on the Discs large protein (Dlg) and anti-HRP staining in the A3 segment muscle 6/7 as indicated. At least 10–15 animals of each genotype were dissected for the bouton analysis. The ANOVA multiple comparison test was used for statistical analysis of the bouton number/muscle.

Eye imaginal disc preparation and analysis

Third instar larvae were dissected and fixed as described previously (Kankel *et al.* 2004). Discs were stained at RT with the following primary antibody in PBS Triton X-100:rabbit anti-TDP43 (Proteintech) at 1:500, and discs were mounted in Vectashield with DAPI. The secondary antibodies used for visualization includes Alexa Fluor 488 goat anti-mouse (green) and Alexa Fluor 594 goat anti-rabbit (red), both at 1:1000 (Invitrogen, Carlsbad, CA).

Microscopy

All confocal images were collected using a Zeiss LSM710 point scanning confocal inverted imaging system using a ×20 and ×40 objective lens. Confocal scanning was performed using the following lasers: 405, 488, and 561 nm. The image acquisition software used was Zeiss Zen (black edition). All samples were mounted and imaged in Vectashield mounting medium supplemented with DAPI (Vector Laboratories) at RT. Adobe Photoshop CS5 was used to further process representative confocal images.

Survival, weight gain, and behavioral testing in mice

Survival data were collected based on either the date of natural death or end stage, which is defined as the age at which mice could no longer right themselves in under 30 S when placed on their back (righting reflex) (Staats *et al.* 2013). Weight and behavior were measured every 10 days starting from P 100 (post natal day 100). The fore and hind limb grip strength test was recorded using the Bioseb instrument by the same technician throughout the whole experiment, and the average strength value (g) of five tests was used for analysis (https://www.bioseb.com/bioseb/anglais/default/item_id=48_Grip-Test.php). The inverted grip strength test was performed as timing the latency that a mouse can hold the grid upside down and the average time (in s) of three tests were documented (Deacon 2013).

Data availability

All reagents and strains described in this study are freely available to the scientific community without any restrictions. The authors affirm that all data necessary for confirming the conclusions of the article are present within the article, figures, and tables. Supplemental material available at figshare: https://doi.org/10.25386/genetics.12202580.

Results

Genetic screen for modifiers of hFUS^{R521C} and hTDP-43^{M337V} photoreceptor degeneration

To explore the genetic circuitry underlying FUS- and TDP43-related activities, we carried out genetic screens (Figure 1A) for modifiers of degenerative eye phenotypes associated with the expression of hTDP-43 or hFUS transgenes carrying fALS-causing mutations. We generated two screening strains *GMR-GAL4*, *UAS-hFUS*^{R521C} (*GMR-hFUS*^{R521C}) and *GMR-GAL4*, *UAS-hTDP-43*^{M337} (*GMR-hTDP-43*^{M337V}) (Figure 1, C and H) and tested their potential to identify *bona fide* ALS-related modifiers by examining whether the strains interact with genes that have been linked to ALS previously. Each strain displayed genetic interactions with the *Drosophila* ortholog of *Senataxin* (*SETX*), *CG7504* or *dSETX*, (Chen *et al.* 2004), *discs overgrown* (*dco*) (Choksi *et al.* 2014), *Hsc70Cb* (Song *et al.* 2013; Nagy *et al.* 2016), and *Apoptotic signal-regulating kinase 1* (*Ask1*) (Fujisawa *et al.* 2016) (Figure 1, D–L). On the basis of these observations we concluded that both strains were suitable to screen for ALS-related modifiers. We note that the Exelixis alleles used throughout the study are in the same genetic background, a genetic background that is distinct from those associated with other publicly available alleles (*e.g.*, *Ask1*^{RNAi}).

We screened the Exelixis Collection of 15,500 insertional mutation strains, which affects ∼50% of the *Drosophila* genome (Artavanis-Tsakonas 2004; Parks *et al.* 2004; Thibault *et al.* 2004) for dominant modification of the photoreceptor degeneration eye phenotypes associated with either of the *GMR-hFUS*^{R521C} or *GMR-hTDP-43*^{M337V} strains (Ritson *et al.* 2010; Lanson *et al.* 2011; Periz *et al.* 2015) (Figure 1A). The Venn diagrams in Figure 2A summarize the results of the screens. We identified 637 and 553 insertions that modified *GMR-hFUS*^{R521C} and *GMR-hTDP-43*^{M337V} phenotypes, respectively (Figure 2A and Table S1). Examples of the effects modifiers have on the *GMR-hFUS*^{R521C} (top panels, Figure 2, B–F and Figure 2, L–O) and *GMR-hTDP-43*^{M337V} (bottom panels, Figure 2, G–K and Figure 2, P–S) screening phenotypes are also shown in Figure 2.

It is important to keep in mind that genetic interactions identified in these screens define hypotheses and thus must be further corroborated. As one focuses on testing hypotheses related to specific modifiers, two caveats of these large-scale screens should be kept in mind. First, it is possible that some of the modifications scored reflect transgene modulation, rather than directly modulate ALS-related phenotype. Second, in some cases the GMR-GAL4 driver may contribute to the modification of the eye phenotypes in an additive or synergistic manner. Determining the specific contribution of the GMR-GAL4 driver to the observed effect for modifiers requires additional testing as there are, surprisingly, inserts that suppress one or both of the screening strains yet enhance the GMR-GAL4 rough-eye phenotype (data not show). However, we note that for the many screens we have carried out using the Exelixis Collection, we found that, in general, if a GAL4

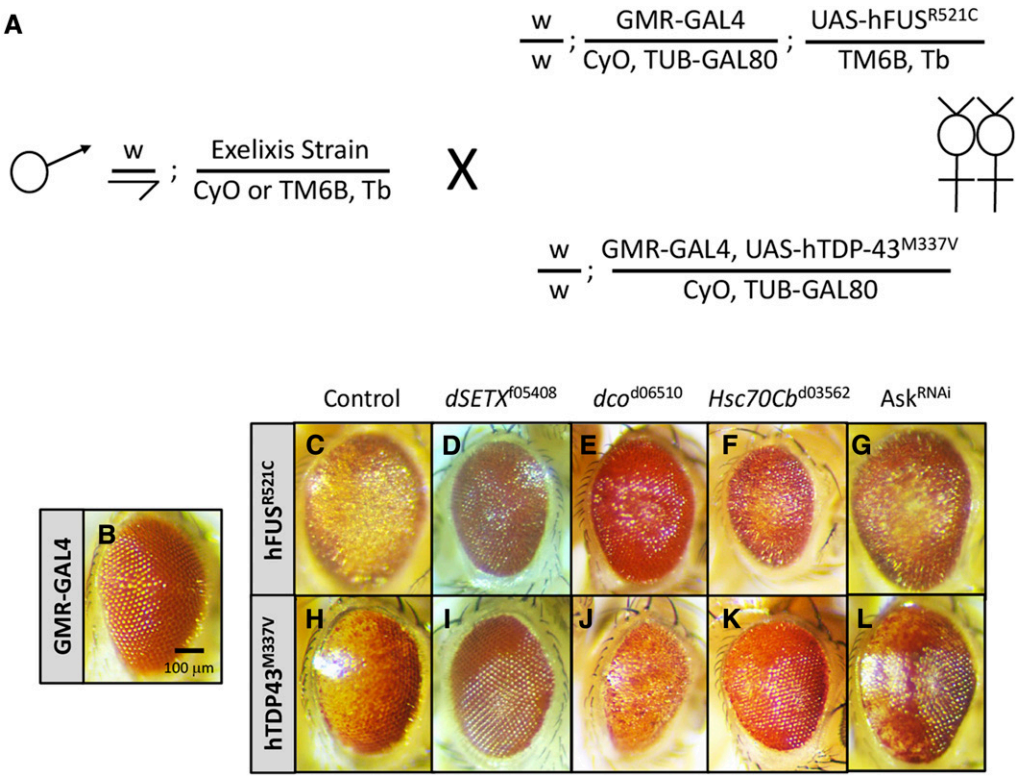

Figure 1 Screening strategy and primary screen validation. (A) Schematic of primary screens for Exelixis insertions that alter degenerative eye phenotypes associated with *w*; *GMR-GAL4*; *UAS-hFUS*^{R521C} (*GMR-hFUS*^{R521C}) and *w*; *GMR-GAL4*, *UAS-hTDP-43*^{M337V} (*GMR-hTDP-43*^{M337V}). These transgenic *Drosophila* models display photoreceptor degeneration/rough-eye phenotypes that are fully penetrant and dosage-sensitive (Ritson *et al.* 2010; Lanson *et al.* 2011; Periz *et al.* 2015). For the primary screen, we generated F1 individuals carrying an Exelixis insertion in *trans* with either *GMR-hFUSR*^{521C} or *GMR-hTDP-43*^{M337V}, which were scored for enhancement or suppression of the eye degeneration phenotype. All primary screen positive inserts were retested in a validation screen using an identical crossing scheme to confirm the initially observed interaction(s). (B) Control *GMR-GAL4* heterozygous individual. The eyes of (C) *GMR-hFUSR*^{521C} and (H) *GMR-hTDP-43*^{M337V} heterozygous animals displaying degenerative, pigmentation, and rough-eye phenotypes. (D–G) *GMR-hFUS*^{R521C} and (I–L) *GMR-hTDP-43*^{M337V} were modulated by Exelixis inserts disrupting genes with known associations to ALS: (D and I) *dSenataxin*^{f05408}, (E and J) *discs overgrown*^{d06510}, (F and K) *Hsc70Cb*^{d03562}, and an (G and L) GAL4-inducible RNAi allele *Ask1*^{32464}. All eyes shown are representative images from individual females. Exelixis stock IDs and *Drosophila* gene symbols are listed, *Ask1*^{RNAi} refers to Bloomington Strain ID (BSID) 32464.

contribution exists, the effects for the overwhelming majority of modifiers is mild, such that suppressors or enhancers can be identified unambiguously (Kankel *et al.* 2007; Chang *et al.* 2008; Hori *et al.* 2011; Pallavi *et al.* 2012; Sen *et al.* 2013).

We found that 205 strains specifically modified *GMR-hFUS*^{R521C} while 121 were specific to *GMR-hTDP-43*^{M337V}. A total of 432 inserts modified both strains (Figure 2A), suggesting considerable commonalities between functional effects of FUS and TDP-43 toxic mutations. The modifiers were further subdivided into specific and common suppressor and enhancer classes of the two screening strains as depicted in Figure 2A (Figure 2A and Table S1). All common enhancer and suppressor strains did affect the FUS and TDP-43 phenotypes in the same manner. However, we also identified 66 insertions (Table S1, column F, "Same modification") not included in the summary Venn diagrams in Figure 2 that acted as an enhancer for one screening strain and as a suppressor for the other. While the underlying mechanism(s) of this differential behavior remains to be determined, it is reasonable to assume that differential modifications reflect underlying functional differences between FUS and TDP-43, which do not display identical pathophysiological behavior in the disease contexts (Kwiatkowski *et al.* 2009a; Vance *et al.* 2009; Mackenzie *et al.* 2010). We finally note that the total number of recovered modifiers represents nearly 5% of the screening library, which is similar to the rate of recovery of genes identified in previous modifier screens using this resource (Kankel *et al.* 2007; Hori *et al.* 2011; Pallavi *et al.* 2012; Sen *et al.* 2013).

Functional classification of modifiers

We used the Gene Ontology (GO) tools at the Panther Classification System (http://www.pantherdb.org/) (Mi *et al.* 2013) to evaluate the biological space encompassed by the gene networks defined in our screens. Panther identified several functional categories in which the predominant terms recovered included "nucleic acid binding," "cytoskeletal protein," "signaling molecule," and "oxidoreductase activity" (data not shown). Members of the most prevalent class (including 64 different genes) identified were annotated as "nucleic acid binding." These include DNA binding proteins and nucleases, but the most abundant subclass (37 different genes) were RBPs (Table S2) (examples shown in Figure 2, L–O and Figure 2, P–S), among which were both suppressors (Figure 2, L, O–R) and enhancers (Figure 2, M, N and S). Notably, 34 out of these 37 genes modified both FUS^{R521C} and TDP-43^{M337V} phenotypes. *Cpsf160* and *RpS2* modified only FUS^{R521C} while *larp* modified only TDP-43^{M337V}. The largest class of RBPs were messenger RNA (mRNA) processing factors (n = 11, of which 9 are involved in mRNA splicing and

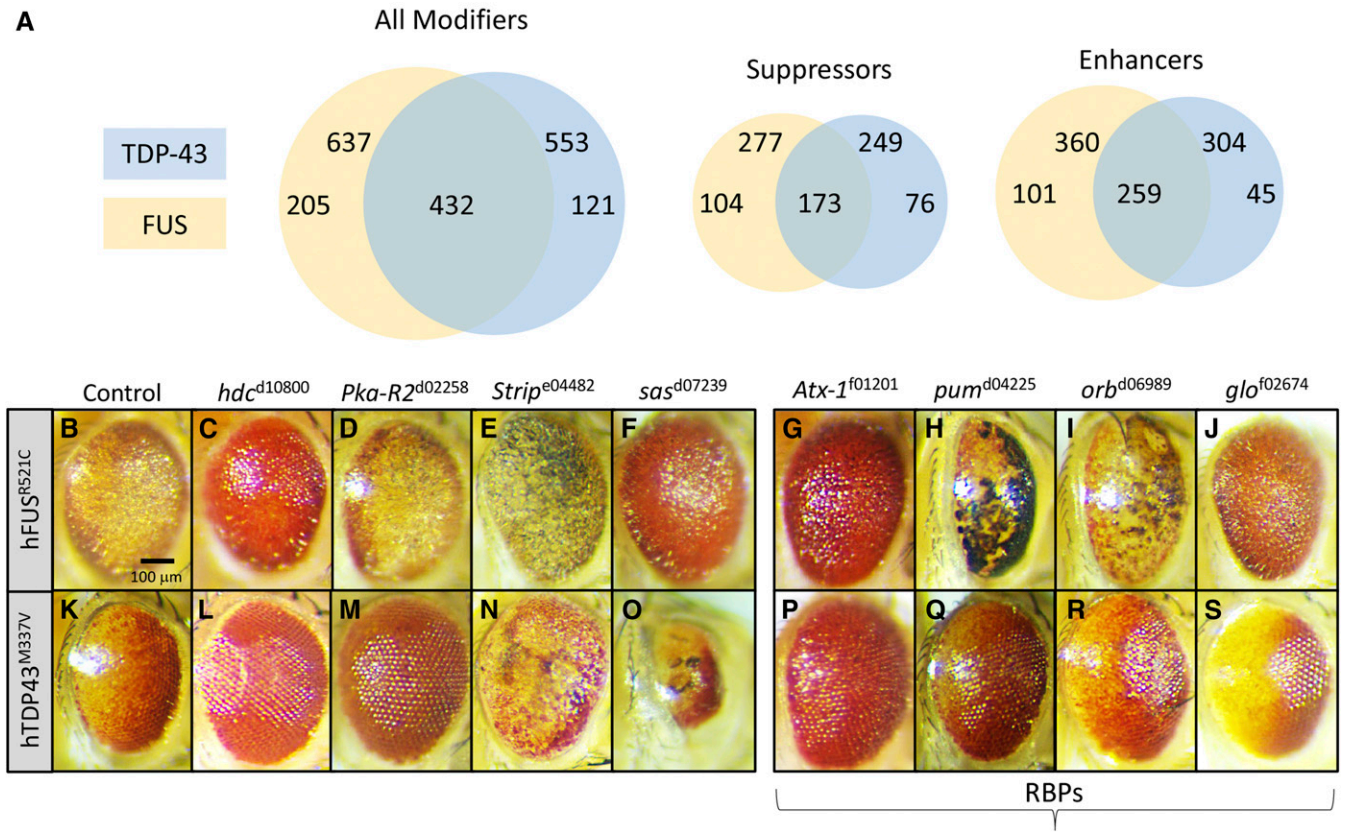

Figure 2 Screen results. (A) Venn diagrams showing the number of validated overlapping inserts with *Drosophila* gene assignments recovered in the screens. In total, 637 *GMR-hFUS*^{R521C} and 553 *GMR-hTDP-43*^{M337V} modifying insertions (enhancers and suppressors) were recovered and validated in each screen, with 432 insertions recovered in both screens. For *GMR-hFUS*^{R521C} 277 suppressors and 360 enhancers were recovered; for *GMR-hTDP-43*^{M337V} the totals were 249 and 304 suppressors and enhancers, respectively, which includes 173 overlapping suppressors and 259 overlapping enhancers. We note that genes recovered in both screens resulting in opposite modification phenotypes were not included in the suppressors and enhancers Venn diagrams. We also note that Table S1 includes all inserts recovered, not only those with clear *Drosophila* gene assignments in the Exelixis Collection. Panels B–S show examples of novel modifiers identified in our screens. Female eyes *trans*-heterozygous *GMR-hFUS*^{R521C} (C–O) and with *GMR-hTDP-43*^{M337V}(H–S) and enhancing or suppressing mutations are shown. *Drosophila* gene symbols and Exelixis Stock IDs are listed. Controls (B and G) demonstrate the eye degeneration phenotype. (C and H) *hdc*^{d10800} suppresses both screening strains, (D) *Pka-R2*^{d02258} has no effect on *GMR-hFUS*^{R521C}, but (I) suppresses *GMR-hTDP-43*^{M337V}, (E and J) *Strip*^{e04482} enhances both screening strains, (F) *sas*^{d07239} suppresses *GMR-hFUS*^{R521C}, and (K) enhances *GMR-hTDP-43*^{M337V}. (L–S) Mutations in different RBPs affect the *GMR-hFUS*^{R521C} and *GMR-hTDP-43*^{M337V} eye phenotypes. (L and P) *Atx-1*^{f01201} suppresses both screening strains, (M and Q) *pum*^{d04225} and (N and R) *orb*^{d06989} enhance *GMR-hFUS*^{R521C} and weakly suppress *GMR-hTDP-43*^{M337V}, and (O and S) *glo*^{f02674} suppresses *GMR-hFUS*^{R521C} and enhances *GMR-hTDP-43*^{M337V}.

2 are mRNA polyadenylation factors) followed by RRM domain containing proteins (n = 10). A noteworthy subclass includes proteins associated with stress granules, which are thought to play a significant role in ALS (Li *et al.* 2013; Lee *et al.* 2016; Markmiller *et al.* 2018). Markmiller *et al.*, have identified ~150 previously unknown human stress granule components using APEX proximity labeling, mass spectrometry, and immunofluorescence (Markmiller *et al.* 2018). Our screens identified the *Drosophila* orthologs of 72 of these novel stress granule genes (data not shown), including several that effected *GMR-hFUS*^{R521C} and *GMR-hTDP-43*^{M337V} (Markmiller *et al.* 2018), as well as a C9ORF72 dipeptide repeat toxicity assay.

A Drosophila c9orf72 ALS model

To further validate the links between a subset of the genes recovered in our screens and ALS-related biology, we developed and utilized secondary assays, based on the premise that modifiers scoring positive in several distinct ALS models more likely point to a common underlying disease mechanism and therefore constitute more promising potential therapeutic targets for sporadic forms of ALS. As the G4C2 hexanucleotide repeat expansion mutations in the *c9orf72* gene represent the most common genetic cause of fALS (Renton *et al.* 2011), we adapted a *c9orf72(G4C2)*$_{30}$ hexanucleotide repeat model of progressive degeneration using the previously described GAL4-inducible *UAS-c9orf72(G4C2)*$_{30}$*-EGFP* transgenic strain (Xu *et al.*) as a secondary assay to corroborate the strongest suppressors identified in the two screens.

GMR-GAL4-driven *UAS-c9orf72(G4C2)*$_{30}$*-EGFP* transgenic (*GMR-c9orf72*$_{30}$) animals displayed progressive degenerative phenotypes over the course of 6 weeks (Figure 3, A–H). Eye

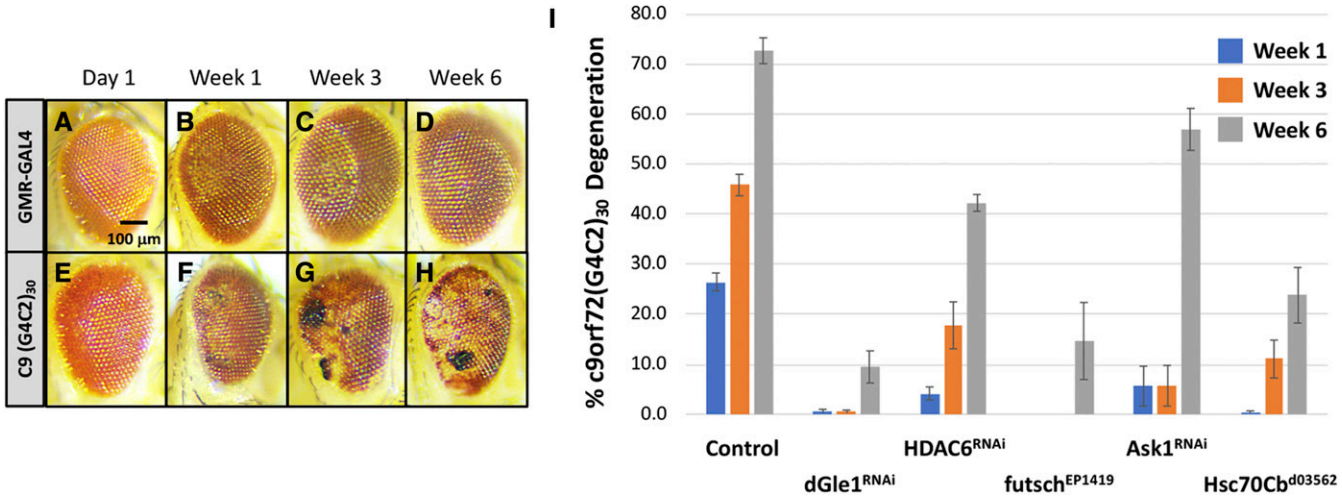

Figure 3 C9ORF72 GGGGCC hexanucleotide repeat model of progressive neurodegeneration. The GAL4-inducible *c9orf72*(G4C2)$_{30}$ transgenic construct was assessed for a progressive neurodegenerative phenotype using the GMR-GAL4 driver over a period of 6 weeks. Neurodegeneration was scored as the presence of black necrotic tissue on the cuticle of the eye. Within a given genotype, the penetrance of neurodegeneration was determined as the fraction of individuals exhibiting black spots within the entire population at multiple time points. Two crosses per genotype were examined and averaged to determine the penetrance of the phenotype. The presence of a single spot on a single eye was considered positive, regardless of the magnitude of the spot(s). (A–D) Representative eye images of aged *GMR-GAL4* individuals display no cuticular photoreceptor degeneration as determined by the presence of black necrotic spots over a period of 6 weeks. (E–H) Representative images of aged *GMR-GAL4*, *UAS-c9orf72*(G4C2)$_{30}$/+ (*GMR-c9orf72$_{30}$*) individuals. Eyes were photographed at day 1 (shortly after hatching), and after 1, 3, and 6 weeks. We note that the darkening of the eye color is an aging effect and does not reflect degeneration. (I) Histogram representation of percent *GMR-c9orf72$_{30}$*/+ individuals (control) displaying the degenerative phenotype at week 1 (blue), week 3 (orange), and week 6 (gray) showing an increase in penetrance of the degenerative phenotype with age. Several genes with established links to ALS are shown to dominantly suppress the *GMR-c9orf72$_{30}$*/+ progressive degeneration validating *GMR-c9orf72$_{30}$* as an ALS-related model. Gene symbols and the Bloomington Stock IDs (BSID) are provided. *dGLE1*^{RNAi}: BSID – 52888, *HDAC6*^{RNAi}: BSID – 31053, *futsch*^{EP1419}: BSID – 10571, *Ask1*^{RNAi}: BSID – 35331 and *Hsc70Cb*^{d03562} is an Exelixis Hsc70Cb allele. The animals of the resulting genotypes were examined: *GMR-c9orf72$_{30}$*/+ (control), *GMR-c9orf72$_{30}$/dGLE1*^{52888} (*dGLE1*^{RNAi}), *GMR-c9orf72$_{30}$*/+; *HDAC6*^{31053}/+ (*HDAC6*^{RNAi}), *futsch*^{EP1419}/+; *GMR-c9orf72$_{30}$*/+ (*futsch*^{EP1419}), *GMR-c9orf72$_{30}$*/+; *Hsc70Cb*^{d03562}/+ (*Hsc70Cb*^{d03562}), and *GMR-c9orf72$_{30}$*/+; *Ask1*^{35331}/+ (*Ask1*^{RNAi}).

degeneration was scored as the presence of one or more black necrotic patches within a single eye; the penetrance of this phenotype increased within the population of *GMR-c9orf72$_{30}$* animals over 6 weeks. Reduced penetrance of the black necrotic tissue at any one of the three time points (weeks 1, 3, or 6) was considered suppression. Figure 3I shows that this progressive degenerative phenotype could indeed be modulated by genes previously linked to ALS, including *CG14749*^{52888} (the *Drosophila* RNA export ortholog of *GLE1: dGLE1*), *HDAC6*^{31053}, *futsch*^{EP1419}, *Ask1*^{35331}, and *Hsc70Cb*^{d03562} (Zhang *et al.* 2008; Song *et al.* 2013; Taes *et al.* 2013; Coyne *et al.* 2014; Freibaum *et al.* 2015; Zhang *et al.* 2015; Fujisawa *et al.* 2016; Nagy *et al.* 2016). We again note that the RNAi and Exelixis strains are in different genetic backgrounds.

We tested 84 of the strongest overlapping *GMR-hFUS*^{R521C} and *GMR-hTDP-43*^{M337V} suppressors in the *GMR-c9orf72$_{30}$* model and identified 56 genes as suppressors, 10 genes as enhancers, and 18 genes that had no detectable effect (Table 1). Among the strongest *GMR-c9orf72$_{30}$* suppressors (suppression at all three time points) was an overexpression allele of *Hsc70Cb*^{d03562}, the *Drosophila* ortholog of *HSPA4L* (Figure 3I). This is noteworthy as Hsc70Cb overexpression suppresses several different *Drosophila* neurodegenerative models (Zhang *et al.* 2010; Kuo *et al.* 2013), while mammalian HSPA4L overexpression provides a survival benefit in two different SOD1 mouse models of ALS (Nagy *et al.* 2016).

Drosophila TDP-43 ALS models

Given that the ALS models used thus far were based on the activities of human transgenes, we decided to corroborate some of our findings using homologous *Drosophila* constructs. We thus generated three transgenic strains harboring the *Drosophila* TDP-43 ortholog (dTDP-43): a strain carrying the wild-type gene (*dTDP-43*^{WT}), a *hTDP-43*^{N378D} cognate disease-associated strain (*dTDP-43*^{N493D}), and a strain harboring a mutation in the NLS (*dTDP-43*^{mNLS}) (Figure S1). Figure 4 shows that GMR-GAL4-directed expression of the *dTDP-43*^{WT} and *dTDP-43*^{mNLS} transgenes caused photoreceptor degeneration in adult animals (Figure 4, A–C), whereas *dTDP-43*^{N493D} expression induced larval lethality (data not shown). We note that, unlike the *GMR-hTDP-43*^{M337V} screening strain, which displays nuclear and cytoplasmic staining and tends to form few detectable aggregates (Figure S2, D and E, see arrows in E), each of these three *Drosophila* transgenic strains exhibited dTDP-43 cytoplasmic mislocalization and aggregate formation in third instar larval eye imaginal discs (Figure 4, D–F). Whether exogenous aggregated dTDP-43 causes endogenous dTDP-43 to mislocalize to the cytoplasm remains to be tested, as the antibody used in these

Table 1 Effects of strongest *GMR-hFUS*^{R521C} and *GMR-hTDP-43*^{M337V} suppressors on *GMR-c9orf72*$(G4C2)_{30}$-related photoreceptor neurodegeneration

Column A Exelixis insert	Column B Fus modification	Column C TDP-43 Modification	Column D C9orf72 Modification	Column E % c9orf72 Degeneration Week 1	Column F % c9orf72 Degeneration Week 3	Column G % c9orf72 Degeneration Week 6
c00800	S2	S3	S3	0	0	1.7
c01016	S2	S2	S3	2.6	12.2	58.5
c01295	S1	S1	S3	6.8	17.6	53.4
c01399	S2	S2	S1	14.2	18.4	50.5
c02909	S1	S2	S3	4.2	10.4	42.4
c03244	S2	S1	S3	8.1	12.9	34.9
c04205	S2	S1	S3	9	14.5	31.8
c04522	S1	S1	S3	0	8.9	46.5
c04582	S2	S2	S2	3.1	26.1	Not done
c05668	S2	S2	S3	1.5	3.1	18.2
c06325	S2	S1	S1	9.4	25.3	64.8
c07023	S2	S3	S3	4.8	9.8	46.1
d00123	S2	S2	S3	0	4.8	0
d00147	S2	S1	S1	4.4	26.1	Not done
d01275	S3	S3	S3	0.7	0.8	0.8
d01345	S2	S2	S3	1.9	9.6	36
d02380	S2	S1	S3	0	3.8	39.6
d02712	S1	S2	S2	7.4	8	70
d02769	S2	S2	S3	0	0	8.3
d02833	S1	S2	S2	0	7.1	Not done
d02874	S1	S1	S1	5.7	45.7	67.6
d03208	S2	S2	S3	0	8.7	6.1
d03562	S3	S3	S3	0.7	7	25.6
d04116	S1	S1	S3	10.8	24	46.2
d04883	S2	S2	S3	5.8	29.8	61.4
d05297	S2	S1	S1	6.6	26.9	Not done
d05884	S2	S1	S2	2.4	28.6	70.3
d06126	S3	S3	S2	8.9	53.4	Not done
d07098	S1	S1	S2	0	16.4	23.4
d08551	S2	S2	S3	0	0	0
d09937	S2	S2	S2	34.5	36.9	62.5
d10223	S2	S3	S2	0	18.4	60
d10376	S3	S2	S3	0	1.2	18.5
d10800	S2	S2	S3	0	0	0
d11666	S2	S2	S3	5.6	9.4	26.5
e00530	S2	S2	S3	0.7	3.3	16.5
e00651	S2	S1	S3	7.3	11.9	44.2
e00985	S2	S2	S3	11.1	20.6	51.6
e01238	S2	S2	S3	1.1	7.1	4
e01976	S2	S2	S3	0	5.9	12.5
e02098	S2	S2	S3	3.4	15.2	43.8
e02166	S2	S2	S1	6.9	37.9	55.2
e02234	S1	S2	S1	15.2	27.7	54.3
e02236	S2	S1	S1	8.2	34.2	59.6
e02284	S3	S3	S3	7	19.1	43.9
e02535	S2	S2	S3	13.5	19.4	67.6
e02684	S2	S1	S2	13.5	30.8	53.9
e02699	S3	S1	S3	7.1	10	29.2
e03409	S2	S2	S1	16.9	20.4	Not done
e04015	S2	S2	S2	0	11.9	27.7
e04545	S2	S2	S3	6.1	13.2	40.2
f01587	S1	S1	S2	10.1	16.5	12.8
f03242	S3	S2	S3	0	0	16.2
f03756	S2	S2	S3	1.3	13	11.1
f05408	S2	S3	S3	0	0	0
f06593	S3	S3	S3	0	0	0
c03600	S2	S2	NE	12.3	26.9	60.9
c04473	S2	S2	NE	18	26.5	65.9

(continued)

Table 1, *continued*

Column A Exelixis insert	Column B Fus modification	Column C TDP-43 Modification	Column D C9orf72 Modification	Column E % c9orf72 Degeneration Week 1	Column F % c9orf72 Degeneration Week 3	Column G % c9orf72 Degeneration Week 6
c04797	S2	S2	NE	24.4	39.3	72.9
c05977	S2	S1	NE	9.2	29.4	Not done
c06293	S2	S2	NE	18.2	34.5	68.5
c06703	S1	S2	NE	32.3	61.1	82.4
c06744	S2	S2	NE	20.1	34.8	63.7
c07042	S1	S1	NE	18.9	40.9	73.3
c07155	S2	S2	NE	22.8	49.4	67.7
d04075	S2	S3	NE	12.4	26.7	Not done
d07488	S2	S2	NE	35.7	30.8	76.9
d08578	S2	S2	NE	26.5	51.5	77.4
d09179	S2	S1	NE	Not done	56.1	72.2
e00355	S2	S2	NE	22.5	31.7	60.3
e00777	S2	S2	NE	15.5	24.9	41.7
e00785	S2	S2	NE	24	32.9	75.6
e02741	S2	S2	NE	27.1	47.5	79
f02738	S1	S1	NE	18.3	22.4	76.8
c03467	S2	S2	E2	41.5	52.5	Not done
c03635	S2	S2	E3	23.6	73.1	95.7
c05849	S2	S1	E1	26.7	57.5	Not done
d02986	S2	S2	E3	13.3	60.2	82.3
d06616	S2	S2	E3	60	80	87.5
e02580	S2	S3	E3	28.4	59	91.5
e04200	S2	S2	E2	66.9	85	Not done
f01201	S2	S2	E3	58.3	78.3	98.2
f03408	S1	S1	E1	20.4	50	77.8
f05963	S1	S2	E3	12.5	68.3	80.8

Effects of 84 overlapping suppressors of *GMR-hFUS*^{R521C} and *GMR-hTDP-43*^{M337V} degenerative eye phenotypes in a *GMR-c9orf72*$(G4C2)_{30}$ model of progressive neurodegeneration. Insert number is listed in Column A, followed by the observed modification in the *GMR-hFUS*^{R521C} (Column B) and *GMR-hTDP-43*^{M337V} (Column C) screening strains. In Columns B and C, S1, S2, and S3 refer to the qualitative strength of suppression, where S1 is weak, S2 is moderate, and S3 is strong suppression. Column D depicts modification effect of the insertion on the *GMR-c9orf72*$(G4C2)_{30}$ model, where S is suppression, E is enhancement, and NE is no effect. Columns E, F, and G provide the penetrance of the neurodegenerative phenotype at weeks 1, 3, and 6. S1/E1 is suppression/enhancement at one time point, S2/E2 is suppression/enhancement at two time points, and S3/E3 is suppression/enhancement at all three time points. Crosses were performed in batches and each insert was compared to control crosses (*GMR-c9orf72*$(G4C2)_{30}$ crossed to isoA) for that particular batch (data not shown).

studies detected only relatively low levels of endogenous dTDP-43 (Figure S2A). Nevertheless, aggregates are considered pathognomonic for ALS, but the disease-related mechanistic relationships of TDP-43 cytoplasmic aggregates to MN dysfunction and degeneration remain unclear. However, our findings are consistent with previous observations where expression of wild-type human and *Drosophila* TDP-43 as well as mutant (A315T) human and *Drosophila* TDP-43 formed cytoplasmic aggregates within the *Drosophila* neuropil (Estes *et al.* 2011). Additionally, moderate overexpression of wild-type hTDP-43 in mice also resulted in intranuclear and cytoplasmic aggregates (Xu *et al.* 2010).

We examined the ability of 16 of the identified modifiers (Table S3) to alter the *GMR-dTDP-43*^{mNLS} eye imaginal disc aggregate formation phenotype. Seven of these modifiers altered the distribution of TDP-43 inclusions (Table S3), resulting in qualitatively fewer aggregates or more diffuse dTDP-43 cytoplasmic staining, whereas the other nine modifiers tested in this assay suppressed the degenerative *GMR-hFUS*^{R521C} and *GMR-hTDP-43*^{M337V} phenotypes, but had no apparent effect on dTDP-43 aggregate formation. We also examined aggregate formation in larval MNs. *OK371-GAL4* larval MN-directed expression of *dTDP-43*^{WT} (Figure 4, G–I), *dTDP-43*^{N493D} (Figure 4, J–L) or *dTDP-43*^{mNLS} (Figure 4, M–O) yielded viable strains, all of which showed various degrees of mislocalized dTDP-43 cytoplasmic aggregates. The formation of cytoplasmic aggregates in *Drosophila* MNs (and eye imaginal discs) are presumably analogous to the documented TDP-43 cytoplasmic aggregation in postmortem patient tissue observed in nearly all forms of ALS (Neumann *et al.* 2006; Ederle and Dormann 2017).

dTDP-43 NMJ morphological defects

Given the relevance of the MN system in ALS, we examined the consequences of MN-directed expression of the *dTDP-43*^{WT}, *dTDP-43*^{mNLS}, and *dTDP-43*^{N493D} transgenic constructs on third larval instar NMJ morphology using two distinct MN drivers: *OK371-GAL4* and *OK6-GAL4* (Figure 5A). By counting the number of boutons per muscle as a proxy for NMJ defects, we found that *OK371-GAL4*, *UAS-dTDP-43*^{N493D} (*OK371-dTDP-43*^{N493D}) animals displayed significant bouton loss, whereas the *dTDP-43*^{WT} and *dTDP-43*^{mNLS} alleles did

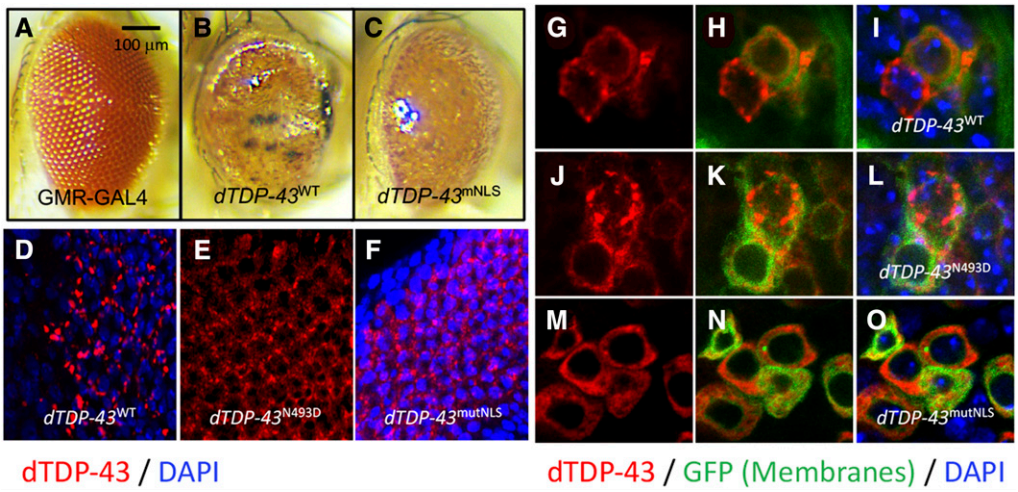

Figure 4 *Drosophila* TDP-43 ALS model. (A–F) Eyes from animals expressing GMR-GAL4 control (A) compared to GMR-dTDP-43^{WT} (B) and GMR-dTDP-43^{mNLS} (C). Expression of each construct results in ommatidia loss and a glossy appearance. GMR-GAL4-driven expression of dTDP-43^{N493D} results in larval lethality. (D–F) Cytoplasmic aggregates are observed in eye discs from individuals with GMR-GAL4-driven (D) wild-type dTDP-43^{WT}, (E) dTDP-43^{N493D}, and (F) dTDP-43^{mNLS} and stained with an antibody directed against human TDP-43 (red); nuclei are stained with DAPI (blue). We note that in control animals relatively low levels of endogenous dTDP-43 expression was detected using this antibody (Figure S2A). (G–O) *OK371-GAL4* drives expression of UAS containing transgenic constructs in larval motor neurons; the *OK371-GAL4* driver strain carries *UAS-CD8-GFP*, which labels the cell membrane of transgene-expressing cells with GFP (green). As above, ectopic dTDP-43 protein is detected with anti-TDP-43 (red) and nuclei are stained with DAPI (blue). (G–I) *UAS-dTDP-43*^{WT} and (J–L) *UAS-dTDP-43*^{N493D} show large cytoplasmic aggregated forms of dTDP-43, with little evidence of more broadly distributed cytoplasmic distributions, whereas (M–O) *UAS-dTDP-43*^{mNLS} exhibits dTDP-43 cytoplasmic mislocalization but appears to produce fewer aggregates and a more diffuse cytoplasmic pattern.

not display any detectable phenotypes when driven by *OK-371-GAL4* (Figure 5, B–E).

To examine whether the NMJ abnormalities associated with *dTDP-43*^{N493D} expression are suitable for further modifier evaluations, we tested three of the strongest suppressors affecting all three ALS photoreceptor degeneration models (*SF2*, *lilli*, and *klp98A*) for their capacities to modify NMJ mutant phenotypes (Figure 5, F–G). We found that the loss-of-function alleles for *SF2*^{32367} and *lilli*^{26314}, but not for *klp98A*^{c05668}, significantly suppressed the *OK371-dTDP-43*^{N493D} NMJ defects as determined by bouton counts (Figure 5H), indicating that the *dTDP-43*^{N493D} NMJ phenotypes offer yet another way to evaluate ALS related modifiers. *SF2* is the *Drosophila* ortholog of mammalian *SRSF1*, which is known to protect against the effects of c9orf72 expansion repeat-dependent phenotypes in *Drosophila* eyes and mammalian cell culture upon its reduction (Hautbergue *et al.* 2017). Furthermore, loss of *lilli* function was recently shown to suppress c9orf72-related phenotypes in *Drosophila* (Yuva-Aydemir *et al.* 2019). In the same study, the authors decreased expression of AFF2/FMR2 (one of four mammalian *lilli* orthologs), which rescued the axonal degeneration and TDP-43 pathology phenotypes in cortical neurons derived from induced pluripotent stem cells of patients with *C9ORF72* mutation (Yuva-Aydemir *et al.* 2019). Consistent with these observations, we determined that reducing *SF2* and *lilli* functions suppressed degeneration induced by *GMR-hFUS*^{R521C}, *GMR-hTDP-43*^{M337V}, and *GMR-c9orf72*$_{30}$ (Figure S3).

Loss of PLD function improves multiple Drosophila ALS phenotypes

Our goal here is not only to define individual ALS modifier genes but, optimally, to identify pathways that are part of the genetic architecture underlying the pathobiology of ALS. In this regard, we were particularly interested in exploring the PLD biochemical pathway as, remarkably, six distinct components of the pathway were identified in our screens as ALS-related modifiers, indicating that PLD activity, and the potential that phosphatidic acid (PA) may play a significant role in modulating ALS-related pathophysiology.

We identified several orthologs of components of the mammalian PLD1/2 pathway as modifiers including *dPld*, *ADP-ribosylation factor GTPase activating protein 3* (*ArfGAP3*), *Phospholipase C at 21C* (*Plc21C*), *Rho1*, *Ras oncogene at 85D* (*Ras85D*), and *Ral guanine nucleotide dissociation stimulator-like* (*Rgl*) (Table S4). RGL, an RalGDS family member, is known to interact with activated Ras as an effector of other Ras family members, such as RalA/B. Upon activation of RalA/B, a number of downstream effectors such as RalBP1 and PLD become activated, leading to a diverse series of biological outcomes (Bodemann and White 2008). We further explored the protective effects of PLD1 downregulation in the context of ALS pathophysiology using an independent GAL4-inducible RNAi *dPld* allele (*dPld*^{32839}). This corroborated the finding that the downregulation of *dPld* suppressed the degenerative phenotypes associated with *GMR-hFUS*^{R521C}, *GMR-hTDP-43*^{M337V}, and *GMR-c9orf72*$_{30}$ (Figure 6, A–E).

Our observations were strengthened by the opposing phenotypic effects displayed by loss- and gain-of-function *dPld* alleles on third instar larval NMJ morphology in *OK371-GAL4* and *OK371-dTDP-43*^{N493D} animals (Figure 6, F–I). In an *OK371-GAL4/+* background, loss of *dPld* function in MNs is without consequence, while MN-directed upregulation of a *UAS-dPld* wild-type transgenic construct significantly worsened NMJ morphology (Figure 6, F–H). We introduced these

A

Drosophila Allele	OK371-GAL4 Expression	OK6-GAL4 Expression
dTDP-43^{WT}	Adults die within 2-3 days after eclosion	Escaper adults die within 2-3 days after eclosion
dTDP-43^{mNLS}	Adults with no obvious defects	Adult flies with no obvious defects
dTDP-43^{N493D}	Wandering/climbing L3, no pupae	L1-L2 lethal, No wandering/climbing L3

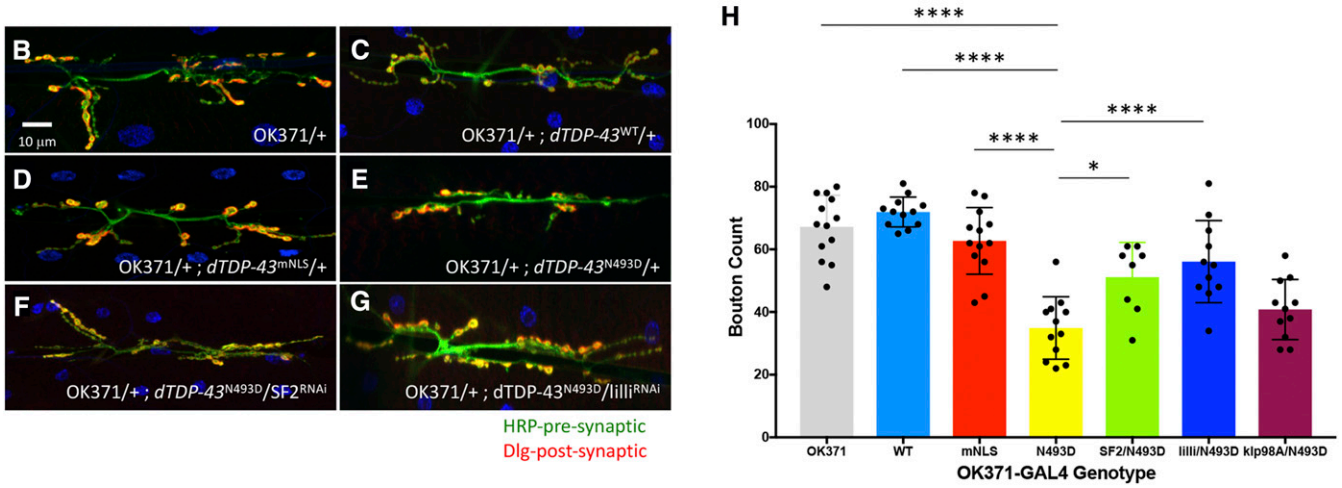

Figure 5 Modifier effects on dTDP-43 transgenic construct expression in the NMJ. (A) Table summarizing the observed phenotypes using two different GAL4 motor neuron drivers (*OK371-GAL4* and *OK6-GAL4*) to direct expression of the following UAS containing transgenic constructs inserted into the ZH-86Fb attB third chromosome insertion site: *dTDP-43*^{WT}, *dTDP-43*^{mNLS}, and *dTDP-43*^{N493D}. (B–G) Qualitative morphological effects on larval NMJs of the following genotypes: (B) *OK371-GAL4*, (C) *OK371-GAL4/+*; *UAS-dTDP-43*^{WT}, (D) *OK371-GAL4/+*; *UAS-dTDP-43*^{mNLS}/+, (E) *OK371-GAL4/+*; *UAS-dTDP-43*^{N493D}/+, (F) *OK371-GAL4/+*; *UAS-dTDP-43*^{N493D}/*SF2*^{32367}, and (G) *OK371-GAL4/+*; *UAS-dTDP-43*^{N493D}/*lilli*^{26314}. (H) Histogram representation of the quantification of the average bouton numbers per muscle in individuals from B–G. All genotypes listed are in an OK371-GAL4/+ background: OK371 are control OK-371-GAL4 heterozygous individuals (gray), WT (light blue), mNLS (red), and N493D (yellow) correspond to the dTDP-43 transgenic constructs, while SF2/N493D (green), lilli/N493D (blue), and klp98A/N493D (magenta) correspond to the *SF2*^{32367}, *lilli*^{26314}, and *klp98A*^{c05668} alleles in the background *OK371-GAL4/+*; *UAS-dTDP-43*^{N493D}. The *dTDP-43*^{N493D} strain displayed significant differences in NMJ bouton counts when compared to *OK371-GAL4* (**** $P < 0.001$), *OK371-GAL4/+*; *UAS-dTDP-43*^{WT} (**** $P < 0.001$), and *OK371-GAL4/+*; *UAS-dTDP-43*^{mNLS} (**** $P < 0.001$). *dTDP-43*^{mNLS} and *dTDP-43*^{WT} bouton numbers were not significantly different from *dTDP-43*^{WT}. SF2 (* $P < 0.0031$) and lilli (**** $P < 0.001$) alleles caused substantial improvement of NMJ morphology in comparison to *OK371-dTDP-43*^{N493D}, while *klp98A* did not. Quantifications were done manually at the confocal microscope and statistical significance was determined by using an unpaired parametric *t*-test with Prism software. NMJ preparations were stained with anti-HRP (green) and anti-discs large (Dlg) (red) to mark pre- and postsynaptic structures, respectively, and muscle nuclei were labeled with DAPI. The asterisks above the lines correspond to the degree of significance between the denoted genotypes. The more asterisks, the smaller the *P*-value.

same loss- and gain-of-function *dPld* alleles into the *OK371-dTDP-43*^{N493D} background to assess whether *dPld* function also affected larval NMJ defects. Consistent with our observations in the eye, loss-of-function *dPld* significantly improved the morphology of the *OK371-dTDP-43*^{N493D} NMJ (Figure 7, G and I), while increasing dPld activity in this context resulted in lethality, with NMJ disorganization so extensive as to preclude bouton quantification.

We further substantiated the involvement of the PLD1 pathway in the suppression of the ALS related phenotypes by examining the effects of *Rgl* (human ortholog: h*Ral-GDS*) and *Rala* modulation (Figure 7, A–I). *Rgl*^{d03208}, which was isolated as a suppressor of the *GMR-hFUS*^{R521C} and *GMR-hTDP-43*^{M337V} eye phenotypes, also suppressed the *GMR-c9orf72*$_{30}$ model of progressive degeneration (Figure S4). We also tested several *Rala* alleles in our ALS models and found that the *Rala*^{34375}-inducible RNAi allele suppressed *GMR-hFUS*^{R521C}, *GMR-hTDP-43*^{M337} and *GMR-c9orf72*$_{30}$ models, while the dominant-negative *Rala*^{32094} allele (Rala^{DN}) suppressed the phenotype in the *GMR-c9orf72*$_{30}$ model (Figure 7, C–H and Figure 7I). Finally, we expressed different *Rgl* and *Rala* GAL4-inducible RNAi alleles (*Rgl*^{28938} and *Rala*^{29850}) in *OK371-dTDP-43*^{N493D} animals and showed that *Rgl* downregulation suppresses the NMJ phenotype associated with this genotype (Figure 7, J–M), in contrast to the *Rala*^{29850} RNAi allele, which had no detectable effect. In summary, these data highlight the role of the PLD pathway in ALS pathophysiology in the *Drosophila* models identifying the pathway as a potential therapeutic target.

Genetic knockout of PLD1/2 function displays modest motor benefits in an SOD1 ALS mouse model

Prompted by our observations in *Drosophila*, the effect of *Pld1*, *Pld2*, and *Pld1/2* ablation was assessed in the widely

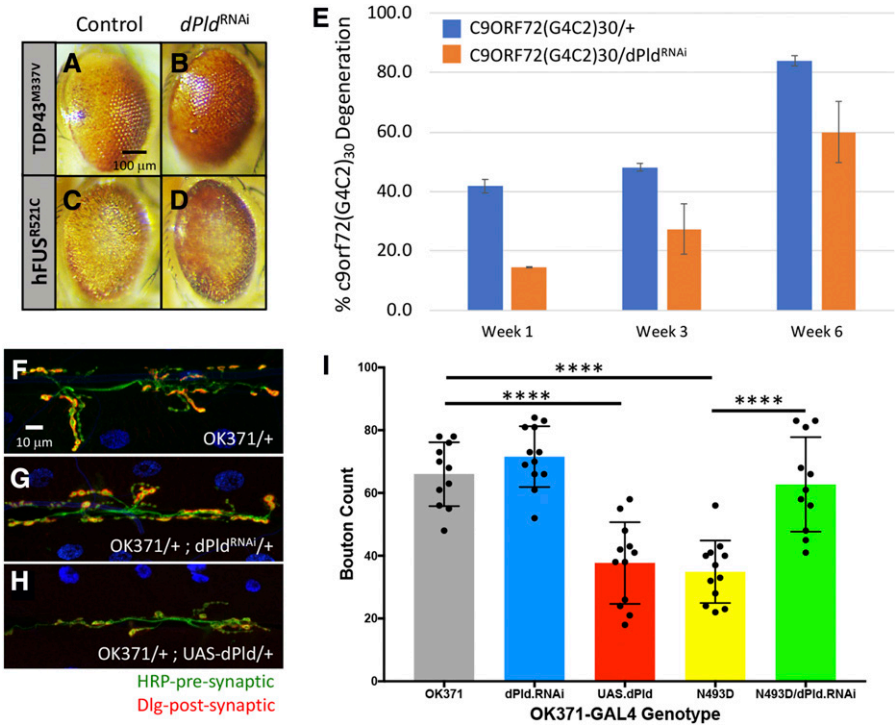

Figure 6 *dPLD* effects on *GMR-hFUS*^{R521C}, *GMR-hTDP-43*^{M337V}, and *GMR-c9orf72*$(G4C2)_{30}$ phenotypes. (A–D) RNAi-induced *dPld* reduction suppressed *GMR-hFUS*^{R521C} and *GMR-hTDP-43*^{M337V} phenotypes. Representative eye images of individuals carrying one copy of (A) *GMR-hTDP-43*^{M337V} in *trans* with (B) *UAS-dPld*^{32839}, or (C) *GMR-hFUSR*^{521C} in *trans* with (D) *UAS-dPld*^{32839}. *dPld*^{32839} expresses an RNAi directed against *dPld*. (E) Histogram representation of percentage of *GMR-c9orf72*$(G4C2)_{30}$ individuals displaying the degenerative phenotype at week 1 (blue), week 3 (orange), and week 6 (gray). GMR-GAL4-directed expression of *UAS-dPld*^{32839} results in suppression of the *c9orf72*$(G4C2)_{30}$-dependent neurodegenerative phenotype at all three time points. (F–H) Effects of motoneuron-driven dPLD on third instar larval NMJ morphology. Representative images of third instar larval NMJs from (F) control *OK371-GAL4* as well as loss [(G) *UAS-dPld*^{32839}] and gain [(H) *UAS-dPld13*] (Raghu *et al.* 2009) of *dPld* function in *OK371-GAL4/+* background are shown. (I) Histogram representation of quantification of average bouton numbers per muscle in *OK371-GAL4* (OK371), *OK371-GAL4/+ UAS-dPld*^{32389}/+ (dPLD.RNAi, gray), *OK371-GAL4/UAS-dPld13* (UAS.dPLD, red), *OK371-GAL4*, *UAS-dTDP-43*^{N493D} (N493D, yellow), and *OK371-GAL4*, *UAS-dTDP-43*^{N493D}/*UAS-dPld*^{32839} (N493D/dPLD.RNAi, green) individuals. Loss of *dPld* has no effect on *OK371-GAL4* bouton number, whereas there is a statistically significant decrease (**** $P < 0.0001$) in bouton number when dPLD is ectopically expressed. Quantifications were done manually at the confocal microscope and statistical significance was determined by using an unpaired parametric *t*-test with Prism software. NMJ preparations were stained with anti-HRP (green) and anti-discs large (Dlg) (red) to mark pre- and postsynaptic structures, respectively, and muscle nuclei were labeled with DAPI. The more asterisks, the smaller the *P*-value.

used, preclinical, SOD1^{G93A} high-copy-number mouse model of ALS (Henriques *et al.* 2010). To this end, mice of three genotypes were generated and analyzed for functional outcomes [hindlimb grip strength, forelimb grip strength, and inverted grip strength, as well as weight gain and survival in SOD1^{G93A} transgenic animals (SOD1^{G93A}; PLD1$-/-$, SOD1^{G93A}; PLD2$-/-$ and SOD1^{G93A}; PLD1$-/-$ and PLD2$-/-$). As depicted in Figure 8, survival (Figure 8A) and weight gain (Figure 8B) were unaffected by elimination of *Pld1*, *Pld2*, or the *Pld1/2* double knockout (all viable: Figure S5) (Sato *et al.* 2013). However, we observed a delay in the onset of functional deficits as measured by grip strength between days 100 and 140 (Figure 8, C, E, and G). The percentage grip strength change was measured between days 100 and 120 for all genotypes. The hindlimb and forelimb grip strength for the wild-type control cohort increased by 20%, whereas the SOD1^{G93A} animals showed a loss for both measurements (Figure 8, D and F; see Figure 8 legend for change in grip strength calculations). In contrast, removal of PLD shows a modest benefit in these parameters, especially obvious when only Pld1 is removed, (Figure 8, D and F). Similarly, in inverted grip strength assays we also observe a modest benefit for all three genotypes compared to SOD1^{G93A} animals (Figure 8H). However, these early benefits are not maintained over the course of disease progression. The functional benefits we observed in the mice appear to be consistent with the loss of *Drosophila dPld* in ALS models that protect NMJ morphology (Figure 6).

We finally note that PLD1 and PLD2 homozygous controls, alone and together, were used as controls for the SOD1+/− mutants with the corresponding PLD1 and/or PLD2 homozygous genotype. The PLD1 and PLD2 littermates were not included as controls since the compound heterozygous SOD1; PLD1 and SOD1; PLD2 animals were not included in our analysis. Our data demonstrate that neither the PLD1 nor PLD2 heterozygous or homozygous knock out animals has a phenotype in terms of MN number, NMJ innervation, and behavior: we observed no difference between wild type, PLD1+/−, PLD2+/−, PLD1−/−, PLD2−/−, and PLD1/2−/− mutants (data not shown). In the absence of a hemizygous PLD1 or PLD2 phenotype, we decided that analysis of the PLD1 and PLD2 heterozygous mutants with or without SOD1 would not contribute further to our study.

Linking Drosophila screens to ALS patient analysis

In an effort to correlate findings from our screens to patient-derived data, we took advantage of a meta-analysis performed by Henderson and colleagues using a published study of postmortem gene expression in MNs from patients with sALS (Rabin *et al.* 2010; Kaplan *et al.* 2014). This analysis identified 41 genes for which high RNA expression levels are correlated with early disease onset. Our screen included 17 of

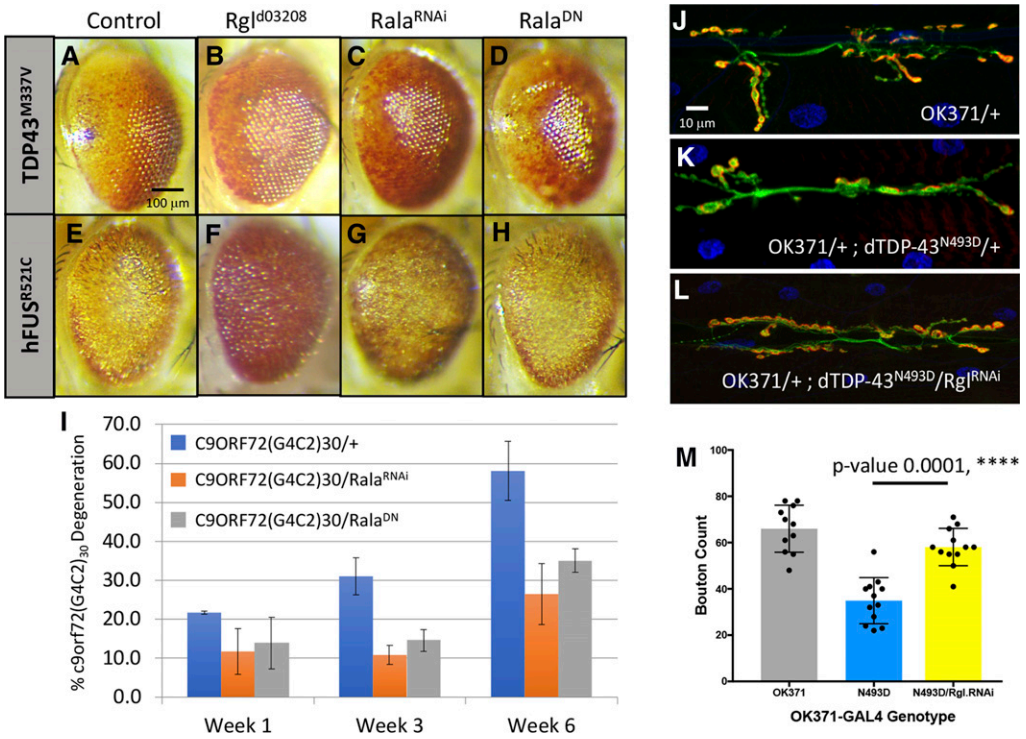

Figure 7 dPLD1 pathway elements modify *Drosophila* ALS models. (A–H) Representative eye images of individuals containing carrying the (A) *GMR-hTDP-43*^{M337V} transgenes in *trans* with (B) *UAS-Rgl*^{d03208}, (C) *UAS-Rala*^{34375} (Rala^{RNAi}), and (D) *UAS-Rala*^{32094} (Rala^{DN}) and the (E) *GMR-hFUS*^{R521C} transgenes in *trans* with (F) *UAS-Rgl*^{d03208}, (G) *UAS-Rala*^{34375} (Rala^{RNAi}), and (H) *UAS-Rala*^{32094} (Rala^{DN}). Both FUS and the TDP-43 phenotypes were suppressed by *Rgl*^{d03208} and *Rala*^{34375} (Rala^{RNAi}). (I) Histogram representation of percentage of individuals displaying the degenerative phenotype at week 1, week 3, and week 6 for (I) *GMR-c9orf72*$(G4C2)_{30}$/+ control (blue), (J) *UAS-Rala*^{34375}/+; *c9orf72*$(G4C2)_{30}$/+ (Rala^{RNAi}) (orange), and *UAS-Rala*^{32094}/+; *c9orf72*$(G4C2)_{30}$/+ (Rala^{DN}) (gray). Both *Rala* alleles strongly suppressed the penetrance of the degenerative c9orf72 phenotype. (J–M) Motor-neuron-directed reduction of *Rgl* affects *OK371-GAL4*; *UAS-dTDP-43*^{N493D}/+ third instar larval NMJ morphology: representative images of control NMJs from (J) *OK371-GAL4* (OK371/+) and (K) *OK371-GAL4*; *UAS-dTDP-43*^{N493D}/+ individuals. (L) The *OK371-GAL4*; *UAS-dTDP-43*^{N493D}/+ NMJ phenotype (K) appears to be qualitatively rescued by RNAi-induced reduction of *Rgl* (*UAS-Rgl*^{28938}) (L). (M) Quantification of average bouton numbers per muscle in individuals of the *OK371-GAL4* (OK371), *OK371-GAL4*; *UAS-dTDP-43*^{N493D}/+ (N493D) and *OK371-GAL4*; *UAS-dTDP-43*^{N493D}/*UAS-Rgl*^{29398} (N493D/Rgl.RNAi) genotypes. RNAi-induced reduction of *Rgl* results in a statistically significant increase in the number of boutons (**** $P < 0.001$). Quantifications were done manually at the confocal microscope and statistical significance was determined by using an unpaired parametric *t*-test with Prism software. NMJ preparations were stained with anti-HRP (green) and anti-discs large (Dlg) (red) to mark pre- and postsynaptic structures, respectively, and muscle nuclei were labeled with DAPI.

these 41 genes as the rest did not have representative alleles in the Exelixis Collection used for the screens. While the functional significance of the increased expression of those genes in ALS is yet to be determined, it is certainly noteworthy that the *Drosophila* orthologs of 11 of these 17 genes were recovered as modifiers of the *GRM-hFUS*^{R521C} and/or *GMR-hTDP-43*^{M337V} models. These genes correspond to the human genes *ARFGAP3*, *CASP3*, *MFN1*, *MFSD1*, *PLD1*, *RAB7L1*, *RALB*, *REL*, *SLC4A7*, *ZNF678*, and *TGFBR1* genes. Moreover, *PLD1*, *RALB*, and *ArfGAP3*, are components of the PLD1 signaling network, consistent with the notion that the PLD1 pathway may be involved in the modulation of ALS phenotypes.

Discussion

Knowledge of the genetic circuitry capable of modulating ALS phenotypes can provide critical insights into ALS-related mechanisms and identify specific gene targets or pathways as potential therapies. Consequently, the generation and validation of experimental tools that allow identification and dissection of genetic interactions underlying ALS-related phenotypes are extremely valuable and important. Given the remarkable conservation of biochemical and developmental pathways across species, our approach is based on the premise that the *Drosophila* orthologs of both TDP-43 and FUS are embedded in genetic pathways that are similar or identical to those of mammals. Identification of genetic modifiers of ALS model phenotypes not only serves to generate testable hypotheses for further understanding the biology associated with ALS pathogenesis, but may also provide additional value by uncovering targets that affect ALS disease progression. A strength of our current study lies in screening the *Drosophila* genome in an unbiased manner for modifiers using two independent ALS models (*GMR-hFUS*^{R521C} and *GMR-hTDP-43*^{M337V}) and validating a subset of the strongest, overlapping suppressors in a third model, *GMR-c9orf72*$_{30}$. Validation across multiple genetic models increases the chance of identifying targets that are relevant to all patients with ALS, including those with sporadic forms of the disease that are clinically indistinguishable from the familial forms.

Functionalities of ALS-related genetic circuitry

The modifiers identified in our screens, included genes previously associated with ALS, validating our approach, as well as a large number of genes that have never before been associated with the disease. The most prevalent class

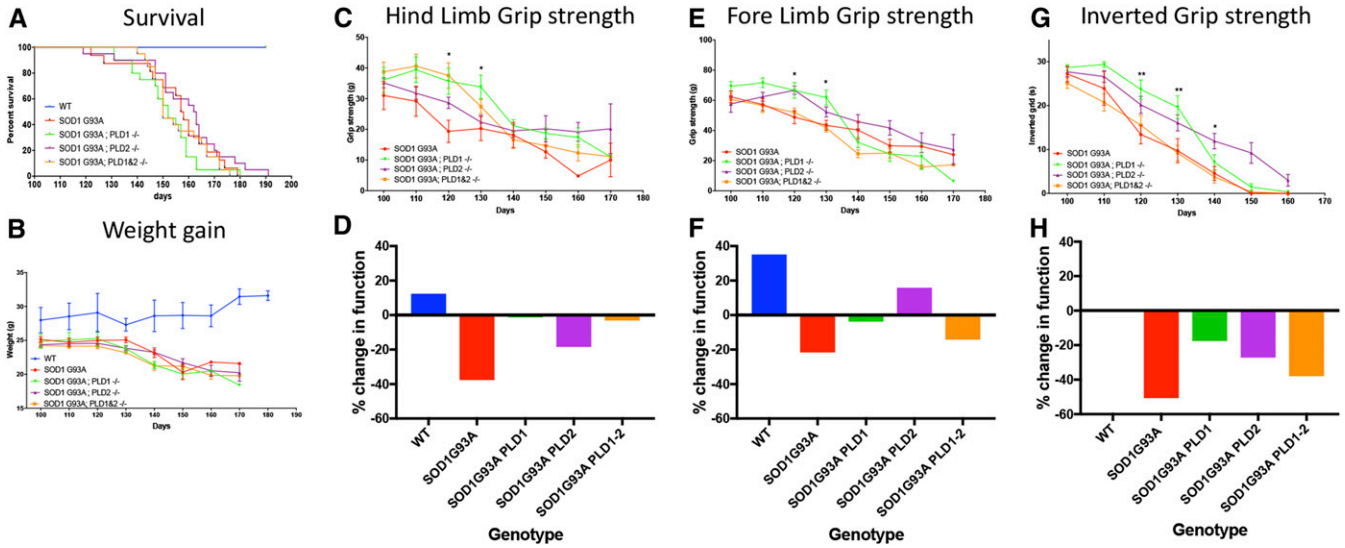

Figure 8 Effects of genetic deletion of PLD in SOD1^{G93A} Mice. Survival, weight, and behavior were measured every 10 days starting from P 100 (post natal day 100). (A) Elimination of PLD1, PLD2, or PLD1/2 combined had no effect on survival of SOD1^{G93A} transgenic animals. (WT (n = 12), SOD1^{G93A} (n = 16), SOD1^{G93A}; PLD1−/− (n = 20), SOD1^{G93A}; PLD2−/− (n = 20) and SOD1^{G93A}; PLD1−/− and PLD2−/− (n = 20) mouse strains). (B) Starting from P 100, mice were weighed every 10 days. PLD1 and/or PLD2 elimination had no effect on the weight loss observed in the SOD1^{G93A} animals. (C and E) Fore limb and hind limb grip strength test measured at P 120 and 130 showed significant improvement of both fore limb and hind limb strength in SOD1^{G93A}; PLD1−/− strains, compared to SOD1^{G93A} controls (* $P < 0.05$, two-way ANOVA, followed by Tukey's multiple comparisons test). In addition, SOD1^{G93A}; PLD2−/− mice had greater fore limb strength and SOD1^{G93A}; PLD1 and PLD2 greater hind limb strength at P 120, compared to the SOD1^{G93A} mice (* $P < 0.05$) (n = 10 in SOD1 group and n = 20 in other groups). (D and F) Percentage change in grip strength from P 100 to P 120 (P 100 value − P 120 value)/P 100 value. Consistent with data in C and E, PLD knockout had mild beneficial effects in terms of fore and hind limb strength. (G and H) Inverted grip strength of the SOD1^{G93A}; PLD1−/− and SOD1^{G93A}; PLD2−/− mice is significantly improved at P 120 and P 130, respectively, compared to the SOD1^{G93A} control animals (* $P < 0.05$ compared to SOD1^{G93A} group, two-way ANOVA, followed by Tukey's multiple comparisons test) (n = 10 in SOD1^{G93A} group and n = 20 in other groups), meanwhile the percentage change was also analyzed and showed similar results.

of modifiers revealed by GO analyses are involved in RNA biology, corroborating its importance in ALS. GO analysis also identified a subset of genes that function in biological pathways associated with ALS pathophysiology, *e.g.*, autophagy, mitochondrial/oxidative stress, apoptosis, neuroinflammation, cytoskeletal, vesicle trafficking, and protein aggregation. This observation agrees with multiple reports that diseases such as ALS, Alzheimer's disease (AD) and Parkinson's disease (PD) share pathophysiological features and cellular dysfunctions, including mitochondrial abnormalities/oxidative stress (Lin and Beal 2006; Liu *et al.* 2017), abnormal RNA biology (King *et al.* 2012; Ramaswami *et al.* 2013), and toxic protein aggregation (Ross and Poirier 2004), which displays transmissibility (Hasegawa *et al.* 2017). Further supporting the notion of commonalities across neurodegenerative diseases, several of the modifiers we identify not only affected our ALS models, but have also been associated with mammalian and *Drosophila* AD-, PD- and Spinal Muscular Atrophy-related models. For instance, the EIF4A1 modifier identified here was also recovered as a modifier in a *Drosophila* Spinal Muscular Atrophy model (Sen *et al.* 2013) and was reported to suppress FUS-dependent proteotoxicity in yeast cells and human HEK293T cells (Sun *et al.* 2011).

Among the many RNA biology-associated genes identified of particular interest are the *Drosophila* orthologs of *SETX* (*dSETX*) and *SRSF1*, *Drosophila SF2*. In humans, mutations in the SETX RNA:DNA helicase lead to a juvenile form of fALS (Chen *et al.* 2004) and ataxia with oculomotor apraxia type 2 (Moreira *et al.* 2004). In addition to *dSETX*, we also identified several other helicases, including DEAD-box helicase 5 (DDX5) and DEAD-box helicase 10 (DDX10). SRSF1, a gene that is involved in multiple aspects of RNA metabolism (Cáceres and Krainer 1993; Zuo and Manley 1993; Huang *et al.* 2004; Sanford *et al.* 2004; Zhang and Krainer 2004; Karni *et al.* 2008; Michlewski *et al.* 2008; Ben-Hur *et al.* 2013; Fregoso *et al.* 2013), modifies c9orf72 repeat expansion-dependent phenotypes through its role in the nuclear cytoplasmic pathway by limiting the nuclear export of c9orf72 transcripts (Hautbergue *et al.* 2017). Consistent with the potential importance of the nucleocytoplasmic pathway in ALS, seven different genes involved in this pathway—the *Drosophila* orthologs of nuclear transport proteins XPO5 and XPO1, the mRNA export gene *GLE1*, as well as core components of the nuclear pore (*i.e.*, Nup88, Nup98, Nup155, and Nup205)—were recovered in our screens. The notion that disruptions to this pathway play a role in disease pathogenesis is consistent with the known cytoplasmic mislocalization of both FUS and TDP-43 proteins associated with ALS

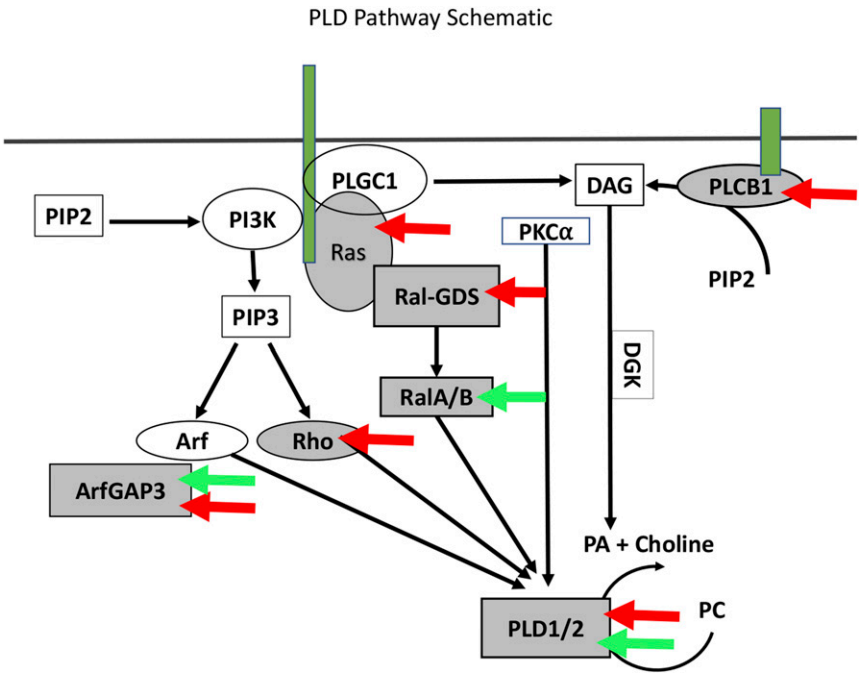

Figure 9 Multiple elements of the PLD1 pathway modify ALS-related phenotypes. Shown is a schematic depicting biochemical relationships leading to Pld production (Foster and Xu 2003). Red arrows point to pathway components identified as modifiers in our *GMR-hFUS*^{R521C} and/or *GMR-hTDP-43*^{M337V} screens. Green arrows point to elements reported to be upregulated in patients with early-onset, but not late-onset, ALS. In both the primary and validation screens six different *Drosophila* orthologs of components of the PLD1 pathway were recovered as modifiers of *GMR-hFUS*^{R521C} and *GMR-hTDP-43*^{M337V}: dPld, ArfGAP3, Rgl, Ras85D, Plc21C, and Rho1, which correspond to the human genes, PLD1, ARFGAP3, RALGDS, KRAS, PLCB1, and RHOA.

pathology, as well as with the finding that TDP-43 pathology disrupts nuclear pore complexes and nucleocytoplasmic transport in ALS/FTD (Freibaum *et al.* 2015; Jovičić *et al.* 2015; Chou *et al.* 2018).

Finally, we note that consistent with several recent studies implicating neuroinflammation in ALS (Chen *et al.* 2018), GO analysis identified NF-κB signaling as a modifier-enriched term. For example, we isolated a putative overexpression allele of *Drosophila* IRAK1 (Interleukin-1 receptor-associated kinase 1), as a strong enhancer of *GMR-hFUS*^{R521C} and *GMR-hTDP-43*^{M337V} phenotypes, raising the possibility that activation of NF-κB through increased activity of IRAK1 may contribute to disease. IRAK1 plays an essential role in the Toll-like receptor pathway by activating NF-κB and mitogen-activated kinases. This is of importance here as OPTN (Chen *et al.* 2018), mutations in which cause fALS, has been shown to bind to IRAK1 and additional data suggested that overexpression of OPTN inhibits IRAK-1-dependent NF-κB activation (Tanishima *et al.* 2017).

Potential therapeutic targets for ALS

A major motivation of our current study was to identify and probe genetic circuits and identify "druggable" targets for potential therapeutics. One modifier that may constitute a target for clinical development is PLD, an enzyme with broad physiological involvement that catalyzes the hydrolysis of phosphatidylcholine into PA and choline. PA acts a second messenger in a broad spectrum of physiological processes (Bruntz *et al.* 2014). Significantly, our studies identified as modifiers several elements of the PLD pathway (Figure 9).

Though PLD1 itself has not been previously linked to ALS, its role in generating PA, which serves as a metabolite for membrane phospholipid biosynthesis, is particularly striking considering the described involvement of lipid metabolic pathways in MN degenerative diseases (Rickman *et al.* 2019). Moreover, PLD activity has been shown to be particularly important in cells under stress conditions while genetic variation in PLD1 has been linked to cancer as well as diverse neurodegenerative diseases, including AD and PD (Chung *et al.* 1995; Sung *et al.* 2001; Yoon *et al.* 2005; Cai *et al.* 2006; Brandenburg *et al.* 2008; Liu *et al.* 2009; Peng and Frohman 2012; Zhu *et al.* 2012; Barclay *et al.* 2013; Bruntz *et al.* 2014; Ammar *et al.* 2015; Rao *et al.* 2015).

The fact that we identified several elements within the entire PLD biochemical cascade as modifiers in our *Drosophila* ALS models presents a strong argument that the pathway may play an important role in modulating ALS disease pathophysiology. Importantly, we also observed phenotypic benefits upon genetic deletion of either *PLD1* or *PLD2*, or both, in the SOD1^{G93A} mouse ALS model, as well as associated elevation in PLD1 levels that correlate with early-onset ALS in human postmortem tissue. Our data therefore support the notion that PLD modulation may have therapeutic consequences for patients with ALS. In *Drosophila*, downregulation of PLD ameliorates degenerative phenotypes in all three ALS models: FUS, TDP-43, and C9ORF72. Whether this is also the case in analogous ALS mouse models remains to be determined.

Two PLD inhibitors are currently available; one is halopemide, which was developed as a neuropsychiatric drug (Bruntz *et al.* 2014; Zhang and Frohman 2014). In limited clinical trials, halopemide had no reported side effects at doses sufficiently high enough to fully block PLD activity (De Cuyper *et al.* 1984). This indicates that PLD inhibition

does not cause major toxicity, even over prolonged periods of time. The second is a halopemide analog, FIPI (Su *et al.* 2009), which acts as a potent inhibitor of both PLD1 and PLD2, with half-life and bioavailability parameters that permit its use in cell culture and animal studies. Further data indicate that FIPI phenocopies outcomes observed in PLD knockout cell lines and animals, as well as in studies using PLD RNAi approaches (Dall'Armi *et al.* 2010; Chen *et al.* 2012; Sanematsu *et al.* 2013; Sato *et al.* 2013; Stegner *et al.* 2013) with no reported off-target effects. Hence, PLD1/2 inhibitors are tolerated in cellular and animal models and apparently satisfy clinical toxicity standards, suggesting that pharmacological inhibition of PLD in patients is likely to be a clinically viable strategy. In this context, it is also noteworthy that the mammalian genome encodes two paralogs, *PLD1* and *PLD2*, and single and double knockouts of both *PLD1* and *PLD2* paralogs in mice are viable (Sato *et al.* 2013).

Given the well-documented role of PLD in AD and PD (Chung *et al.* 1995; Sung *et al.* 2001; Yoon *et al.* 2005; Cai *et al.* 2006; Brandenburg *et al.* 2008; Liu *et al.* 2009; Peng and Frohman 2012; Zhu *et al.* 2012; Barclay *et al.* 2013; Bruntz *et al.* 2014; Ammar *et al.* 2015; Rao *et al.* 2015), and our implication of PLD activity in ALS pathophysiology, it is conceivable that the PLD pathway plays a more central role in neurodegeneration. It will certainly be worth testing the efficacy of halopemide and FIPI in ALS murine models. Positive results in such experiments, in combination with the human and animal model data described here, could warrant a full-scale clinical development program for halopemide and/or FIPI as ALS therapeutics. However, given the modest benefit in the $SOD1^{G93A}$ mouse model resulting from genetic deletion of the PLD pathway, PLD inhibition alone may not provide significant benefit to patients with ALS. Instead, it is worth considering the possibility that PLD inhibition might be deployed in the context of a combinatorial therapeutic approach in which, for instance, a causative gene is also targeted.

In conclusion, our study highlights the advantages of *Drosophila* models for the identification of functional circuitries within which individual disease genes are embedded. *Drosophila*, as well as other invertebrate models, offer unique advantages for the dissection of such circuitries, notwithstanding the fact that observations from these systems must be validated in mammalian/human contexts. Nevertheless, the links we have identified via genetic screens allow us to formulate hypotheses regarding underlying molecular mechanisms that can be tested in preclinical models, offering the possibility to identify novel therapeutic targets or indeed biomarkers of interest.

Acknowledgments

We thank Angeliki Louvi, Diana M. Ho, and Marc Muskavitch for their valuable comments on the manuscript. We also thank Glenn Doughty, Mark Godek, and Dexter Bidot for providing us with the Exelixis strains and supplying vast amounts of fly food that enabled us to perform the screens. We also appreciate the efforts of Ramiro Massol at the Biogen Imaging Center for his help. The *UAS-dPld13* was a generous gift of Dr. Raghu Padinjat. This work was supported by a sponsored research agreement provided to Dr. Artavanis-Tsakonas by Biogen. Dr Artavanis-Tsakonas maintains a visiting scientist role at Biogen and owns Biogen stock.

Literature Cited

Abe, K., M. Aoki, S. Tsuji, Y. Itoyama, G. Sobue *et al.*, 2017 Safety and efficacy of edaravone in well defined patients with amyotrophic lateral sclerosis: a randomised, double-blind, placebo-controlled trial. Lancet Neurol. 16: 505–512. https://doi.org/10.1016/S1474-4422(17)30115-1

Ammar, M. R., T. Thahouly, A. Hanauer, D. Stegner, B. Nieswandt *et al.*, 2015 PLD1 participates in BDNF-induced signalling in cortical neurons. Sci. Rep. 5: 14778. https://doi.org/10.1038/srep14778

Andersson, M. K., A. Stahlberg, Y. Arvidsson, A. Olofsson, H. Semb *et al.*, 2008 The multifunctional FUS, EWS and TAF15 proto-oncoproteins show cell type-specific expression patterns and involvement in cell spreading and stress response. BMC Cell Biol. 9: 37. https://doi.org/10.1186/1471-2121-9-37

Arai, T., M. Hasegawa, H. Akiyama, K. Ikeda, T. Nonaka *et al.*, 2006 TDP-43 is a component of ubiquitin-positive tau-negative inclusions in frontotemporal lobar degeneration and amyotrophic lateral sclerosis. Biochem. Biophys. Res. Commun. 351: 602–611. https://doi.org/10.1016/j.bbrc.2006.10.093

Artavanis-Tsakonas, S., 2004 Accessing the exelixis collection. Nat. Genet. 36: 207. https://doi.org/10.1038/ng1316

Ayala, Y. M., P. Zago, A. D'Ambrogio, Y. F. Xu, L. Petrucelli *et al.*, 2008 Structural determinants of the cellular localization and shuttling of TDP-43. J. Cell Sci. 121: 3778–3785. https://doi.org/10.1242/jcs.038950

Barclay, Z., L. Dickson, D. Robertson, M. Johnson, P. Holland *et al.*, 2013 Attenuated PLD1 association and signalling at the H452Y polymorphic form of the 5-HT(2A) receptor. Cell. Signal. 25: 814–821. https://doi.org/10.1016/j.cellsig.2013.01.004

Ben-Hur, V., P. Denichenko, Z. Siegfried, A. Maimon, A. Krainer *et al.*, 2013 S6K1 alternative splicing modulates its oncogenic activity and regulates mTORC1. Cell Rep. 3: 103–115. https://doi.org/10.1016/j.celrep.2012.11.020

Bischof, J., M. Bjorklund, E. Furger, C. Schertel, J. Taipale *et al.*, 2013 A versatile platform for creating a comprehensive UAS-ORFeome library in Drosophila. Development 140: 2434–2442. https://doi.org/10.1242/dev.088757

Bodemann, B. O., and M. A. White, 2008 Ral GTPases and cancer: linchpin support of the tumorigenic platform. Nat. Rev. Cancer 8: 133–140. https://doi.org/10.1038/nrc2296

Brandenburg, L. O., M. Konrad, C. Wruck, T. Koch, T. Pufe *et al.*, 2008 Involvement of formyl-peptide-receptor-like-1 and phospholipase D in the internalization and signal transduction of amyloid beta 1–42 in glial cells. Neuroscience 156: 266–276. https://doi.org/10.1016/j.neuroscience.2008.07.042

Brown, R. H., and A. Al-Chalabi, 2017 Amyotrophic lateral sclerosis. N. Engl. J. Med. 377: 162–172. https://doi.org/10.1056/NEJMra1603471

Bruntz, R. C., C. W. Lindsley, and H. A. Brown, 2014 Phospholipase D signaling pathways and phosphatidic acid as therapeutic targets in cancer. Pharmacol. Rev. 66: 1033–1079. https://doi.org/10.1124/pr.114.009217

Bunton-Stasyshyn, R. K., R. A. Saccon, P. Fratta, and E. M. Fisher, 2015 SOD1 function and its implications for amyotrophic

lateral sclerosis pathology: new and renascent themes. Neuroscientist 21: 519–529. https://doi.org/10.1177/1073858414561795
Buratti, E., and F. E. Baralle, 2001 Characterization and functional implications of the RNA binding properties of nuclear factor TDP-43, a novel splicing regulator of CFTR exon 9. J. Biol. Chem. 276: 36337–36343. https://doi.org/10.1074/jbc.M104236200
Byrne, S., C. Walsh, C. Lynch, P. Bede, M. Elamin *et al.*, 2011 Rate of familial amyotrophic lateral sclerosis: a systematic review and meta-analysis. J. Neurol. Neurosurg. Psychiatry 82: 623–627. https://doi.org/10.1136/jnnp.2010.224501
Cáceres, J. F., and A. R. Krainer, 1993 Functional analysis of pre-mRNA splicing factor SF2/ASF structural domains. EMBO J. 12: 4715–4726. https://doi.org/10.1002/j.1460-2075.1993.tb06160.x
Cai, D., M. Zhong, R. Wang, W. J. Netzer, D. Shields *et al.*, 2006 Phospholipase D1 corrects impaired betaAPP trafficking and neurite outgrowth in familial Alzheimer's disease-linked presenilin-1 mutant neurons. Proc. Natl. Acad. Sci. USA 103: 1936–1940. https://doi.org/10.1073/pnas.0510710103
Chang, H. C., D. N. Dimlich, T. Yokokura, A. Mukherjee, M. W. Kankel *et al.*, 2008 Modeling spinal muscular atrophy in Drosophila. PLoS One 3: e3209. https://doi.org/10.1371/journal.pone.0003209
Chen, Y. Z., C. L. Bennett, H. M. Huynh, I. P. Blair, I. Puls *et al.*, 2004 DNA/RNA helicase gene mutations in a form of juvenile amyotrophic lateral sclerosis (ALS4). Am. J. Hum. Genet. 74: 1128–1135. https://doi.org/10.1086/421054
Chen, Q., T. Hongu, T. Sato, Y. Zhang, W. Ali *et al.*, 2012 Key roles for the lipid signaling enzyme phospholipase d1 in the tumor microenvironment during tumor angiogenesis and metastasis. Sci. Signal. 5: ra79. https://doi.org/10.1126/scisignal.2003257
Chen, H., M. W. Kankel, S. C. Su, S. W. S. Han, and D. Ofengeim, 2018 Exploring the genetics and non-cell autonomous mechanisms underlying ALS/FTLD. Cell Death Differ. 25: 648–660. https://doi.org/10.1038/s41418-018-0060-4
Chenna, R., 2003 Multiple sequence alignment with the Clustal series of programs. Nucleic Acids Res. 31: 3497–3500. https://doi.org/10.1093/nar/gkg500
Choksi, D. K., B. Roy, S. Chatterjee, T. Yusuff, M. F. Bakhoum *et al.*, 2014 TDP-43 phosphorylation by casein kinase Iε promotes oligomerization and enhances toxicity in vivo. Hum. Mol. Genet. 23: 1025–1035. https://doi.org/10.1093/hmg/ddt498
Chou, C. C., Y. Zhang, M. E. Umoh, S. W. Vaughan, I. Lorenzini *et al.*, 2018 TDP-43 pathology disrupts nuclear pore complexes and nucleocytoplasmic transport in ALS/FTD. Nat. Neurosci. 21: 228–239. https://doi.org/10.1038/s41593-017-0047-3
Chung, S. Y., T. Moriyama, E. Uezu, K. Uezu, R. Hirata *et al.*, 1995 Administration of phosphatidylcholine increases brain acetylcholine concentration and improves memory in mice with dementia. J. Nutr. 125: 1484–1489.
Coyne, A. N., B. B. Siddegowda, P. S. Estes, J. Johannesmeyer, T. Kovalik *et al.*, 2014 Futsch/MAP1B mRNA is a translational target of TDP-43 and is neuroprotective in a Drosophila model of amyotrophic lateral sclerosis. J. Neurosci. 34: 15962–15974. https://doi.org/10.1523/JNEUROSCI.2526-14.2014
Crozat, A., P. Aman, N. Mandahl, and D. Ron, 1993 Fusion of CHOP to a novel RNA-binding protein in human myxoid liposarcoma. Nature 363: 640–644. https://doi.org/10.1038/363640a0
Daigle, J. G., N. A. Lanson, Jr., R. B. Smith, I. Casci, A. Maltare *et al.*, 2013 RNA-binding ability of FUS regulates neurodegeneration, cytoplasmic mislocalization and incorporation into stress granules associated with FUS carrying ALS-linked mutations. Hum. Mol. Genet. 22: 1193–1205. https://doi.org/10.1093/hmg/dds526
Dall'Armi, C., A. Hurtado-Lorenzo, H. Tian, E. Morel, A. Nezu *et al.*, 2010 The phospholipase D1 pathway modulates macroautophagy. Nat. Commun. 1: 142. https://doi.org/10.1038/ncomms1144
De Cuyper, H., H. M. van Praag, and D. Verstraeten, 1984 The clinical significance of halopemide, a dopamine-blocker related to the butyrophenones. Neuropsychobiology 12: 211–216. https://doi.org/10.1159/000118141
Deacon, R. M., 2013 Measuring the strength of mice. J. Vis. Exp. (76), e2610. https://doi.org/10.3791/2610
Deng, H., K. Gao, and J. Jankovic, 2014 The role of FUS gene variants in neurodegenerative diseases. Nat. Rev. Neurol. 10: 337–348. https://doi.org/10.1038/nrneurol.2014.78
Ederle, H., and D. Dormann, 2017 TDP-43 and FUS en route from the nucleus to the cytoplasm. FEBS Lett. 591: 1489–1507. https://doi.org/10.1002/1873-3468.12646
Estes, P. S., A. Boehringer, R. Zwick, J. E. Tang, B. Grigsby *et al.*, 2011 Wild-type and A315T mutant TDP-43 exert differential neurotoxicity in a Drosophila model of ALS. Hum. Mol. Genet. 20: 2308–2321. https://doi.org/10.1093/hmg/ddr124
Feiguin, F., V. K. Godena, G. Romano, A. D'Ambrogio, R. Klima *et al.*, 2009 Depletion of TDP-43 affects Drosophila motoneurons terminal synapsis and locomotive behavior. FEBS Lett. 583: 1586–1592. https://doi.org/10.1016/j.febslet.2009.04.019
Foster, D. A., and L. Xu, 2003 Phospholipase D in cell proliferation and cancer. Mol. Cancer Res. 1: 789–800.
Fregoso, O. I., S. Das, M. Akerman, and A. R. Krainer, 2013 Splicing-factor oncoprotein SRSF1 stabilizes p53 via RPL5 and induces cellular senescence. Mol. Cell 50: 56–66. https://doi.org/10.1016/j.molcel.2013.02.001
Freibaum, B., Y. Lu, R. Lopez-Gonzalez, N. C. Kim, S. Almeida *et al.*, 2015 GGGGCC repeat expansion in C9orf72 compromises nucleocytoplasmic transport. Nature 525: 129–133. https://doi.org/10.1038/nature14974
Fujisawa, T., M. Takahashi, Y. Tsukamoto, N. Yamaguchi, M. Nakoji *et al.*, 2016 The ASK1-specific inhibitors K811 and K812 prolong survival in a mouse model of amyotrophic lateral sclerosis. Hum. Mol. Genet. 25: 245–253. https://doi.org/10.1093/hmg/ddv467
Ghasemi, M., and R. H. Brown, Jr., 2018 Genetics of amyotrophic lateral sclerosis. Cold Spring Harb. Perspect. Med. 8: a024125. https://doi.org/10.1101/cshperspect.a024125
Gibson, S. B., J. M. Downie, S. Tsetsou, J. E. Feusier, K. P. Figueroa *et al.*, 2017 The evolving genetic risk for sporadic ALS. Neurology 89: 226–233. https://doi.org/10.1212/WNL.0000000000004109
Goodman, L. D., and N. M. Bonini, 2020 New roles for canonical transcription factors in repeat expansion diseases. Trends Genet. 36: 81–92. https://doi.org/10.1016/j.tig.2019.11.003
Gros-Louis, F., C. Gaspar, and G. A. Rouleau, 2006 Genetics of familial and sporadic amyotrophic lateral sclerosis. Biochim. Biophys. Acta 1762: 956–972. https://doi.org/10.1016/j.bbadis.2006.01.004
Guruharsha, K. G., J. F. Rual, B. Zhai, J. Mintseris, P. Vaidya *et al.*, 2011 A protein complex network of Drosophila melanogaster. Cell 147: 690–703. https://doi.org/10.1016/j.cell.2011.08.047
Hardiman, O., and L. H. van den Berg, 2017 Edaravone- a new treatment for ALS on the horizon? Lancet Neurol. 16: 490–491. https://doi.org/10.1016/S1474-4422(17)30163-1
Hasegawa, M., T. Nonaka, and M. Masuda-Suzukake, 2017 Prion-like mechanisms and potential therapeutic targets in neurodegenerative disorders. Pharmacol. Ther. 172: 22–33. https://doi.org/10.1016/j.pharmthera.2016.11.010
Hautbergue, G. M., L. M. Castelli, L. Ferraiuolo, A. Sanchez-Martinez, J. Cooper-Knock *et al.*, 2017 SRSF1-dependent nuclear export inhibition of C9ORF72 repeat transcripts prevents neurodegeneration and associated motor deficits. Nat. Commun. 8: 16063. https://doi.org/10.1038/ncomms16063

Henriques, A., C. Pitzer, and A. Schneider, 2010 Characterization of a novel SOD-1(G93A) transgenic mouse line with very decelerated disease development. PLoS One 5: e15445. https://doi.org/10.1371/journal.pone.0015445

Hori, K., A. Sen, T. Kirchhausen, and S. Artavanis-Tsakonas, 2011 Synergy between the ESCRT-III complex and Deltex defines a ligand-independent Notch signal. J. Cell Biol. 195: 1005–1015. https://doi.org/10.1083/jcb.201104146

Huang, Y., S. Dey, X. Zhang, F. Sonnichsen, and P. Garner, 2004 The alpha-helical peptide nucleic acid concept: merger of peptide secondary structure and codified nucleic acid recognition. J. Am. Chem. Soc. 126: 4626–4640. https://doi.org/10.1021/ja038434s

Hu, Y., I. Flockhart, A. Vinayagam, C. Bergwitz, B. Berger *et al.*, 2011 An integrative approach to ortholog prediction for disease-focused and other functional studies. BMC Bioinformatics 12: 357. https://doi.org/10.1186/1471-2105-12-357

Iko, Y., T. S. Kodama, N. Kasai, T. Oyama, E. H. Morita *et al.*, 2004 Domain architectures and characterization of an RNA-binding protein, TLS. J. Biol. Chem. 279: 44834–44840. https://doi.org/10.1074/jbc.M408552200

Ito, D., M. Hatano, and N. Suzuki, 2017 RNA binding proteins and the pathological cascade in ALS/FTD neurodegeneration. Sci. Transl. Med. 9: eaah5436. https://doi.org/10.1126/scitranslmed.aah5436

Joviččić, A., J. Mertens, S. Boeynaems, E. Bogaert, N. Chai *et al.*, 2015 Modifiers of C9orf72 dipeptide repeat toxicity connect nucleocytoplasmic transport defects to FTD/ALS. Nat. Neurosci. 18: 1226–1229. https://doi.org/10.1038/nn.4085

Kankel, M. W., D. M. Duncan, and I. Duncan, 2004 A screen for genes that interact with the Drosophila pair-rule segmentation gene fushi tarazu. Genetics 168: 161–180. https://doi.org/10.1534/genetics.104.027250

Kankel, M. W., G. D. Hurlbut, G. Upadhyay, V. Yajnik, B. Yedvobnick *et al.*, 2007 Investigating the genetic circuitry of mastermind in Drosophila, a notch signal effector. Genetics 177: 2493–2505. https://doi.org/10.1534/genetics.107.080994

Kaplan, A., K. J. Spiller, C. Towne, K. C. Kanning, G. T. Choe *et al.*, 2014 Neuronal matrix metalloproteinase-9 is a determinant of selective neurodegeneration. Neuron 81: 333–348. https://doi.org/10.1016/j.neuron.2013.12.009

Karni, R., Y. Hippo, S. W. Lowe, and A. R. Krainer, 2008 The splicing-factor oncoprotein SF2/ASF activates mTORC1. Proc. Natl. Acad. Sci. USA 105: 15323–15327. https://doi.org/10.1073/pnas.0801376105

Kato, M., T. W. Han, S. Xie, K. Shi, X. Du *et al.*, 2012 Cell-free formation of RNA granules: low complexity sequence domains form dynamic fibers within hydrogels. Cell 149: 753–767. https://doi.org/10.1016/j.cell.2012.04.017

King, O. D., A. D. Gitler, and J. Shorter, 2012 The tip of the iceberg: RNA-binding proteins with prion-like domains in neurodegenerative disease. Brain Res. 1462: 61–80. https://doi.org/10.1016/j.brainres.2012.01.016

Kuo, Y., S. Ren, U. Lao, B. A. Edgar, and T. Wang, 2013 Suppression of polyglutamine protein toxicity by co-expression of a heat-shock protein 40 and a heat-shock protein 110. Cell Death Dis. 4: e833. https://doi.org/10.1038/cddis.2013.351

Kwiatkowski, T. J., Jr., D. A. Bosco, A. L. Leclerc, E. Tamrazian, C. R. Vanderburg *et al.*, 2009a Mutations in the FUS/TLS gene on chromosome 16 cause familial amyotrophic lateral sclerosis. Science 323: 1205–1208. https://doi.org/10.1126/science.1166066

Kwiatkowski, T. J. J., D. A. Bosco, A. L. LeClerc, E. Tamrazian, C. R. Vanderburg *et al.*, 2009b Mutations in the FUS/TLS gene on chromosome 16 cause familial amyotrophic Lateral sclerosis. Science 323: 1205–1208. https://doi.org/10.1126/science.1166066

Lagier-Tourenne, C., M. Polymenidou, and D. W. Cleveland, 2010 TDP-43 and FUS/TLS: emerging roles in RNA processing and neurodegeneration. Hum. Mol. Genet. 19: R46–R64. https://doi.org/10.1093/hmg/ddq137

Lanson, N. A., Jr., A. Maltare, H. King, R. Smith, J. H. Kim *et al.*, 2011 A Drosophila model of FUS-related neurodegeneration reveals genetic interaction between FUS and TDP-43. Hum. Mol. Genet. 20: 2510–2523. https://doi.org/10.1093/hmg/ddr150

Larkin, M. A., G. Blackshields, N. P. Brown, R. Chenna, P. A. McGettigan *et al.*, 2007 Clustal W and clustal X version 2.0. Bioinformatics 23: 2947–2948. https://doi.org/10.1093/bioinformatics/btm404

Lee, K. H., P. Zhang, H. J. Kim, D. M. Mitrea, M. Sarkar *et al.*, 2016 C9orf72 dipeptide repeats impair the assembly, dynamics, and function of membrane-less organelles. Cell 167: 774–788.e17. https://doi.org/10.1016/j.cell.2016.10.002

Li, Y., P. Ray, E. J. Rao, C. Shi, W. Guo *et al.*, 2010 A Drosophila model for TDP-43 proteinopathy. Proc. Natl. Acad. Sci. USA 107: 3169–3174. https://doi.org/10.1073/pnas.0913602107

Li, Y. R., O. D. King, J. Shorter, and A. D. Gitler, 2013 Stress granules as crucibles of ALS pathogenesis. J. Cell Biol. 201: 361–372. https://doi.org/10.1083/jcb.201302044

Lin, M. T., and M. F. Beal, 2006 Mitochondrial dysfunction and oxidative stress in neurodegenerative diseases. Nature 443: 787–795. https://doi.org/10.1038/nature05292

Lin, M. J., C. W. Cheng, and C. K. Shen, 2011 Neuronal function and dysfunction of Drosophila dTDP. PLoS One 6: e20371. https://doi.org/10.1371/journal.pone.0020371

Ling, S. C., M. Polymenidou, and D. W. Cleveland, 2013 Converging mechanisms in ALS and FTD: disrupted RNA and protein homeostasis. Neuron 79: 416–438. https://doi.org/10.1016/j.neuron.2013.07.033

Liu, Y., Y. W. Zhang, X. Wang, H. Zhang, X. You *et al.*, 2009 Intracellular trafficking of presenilin 1 is regulated by β-amyloid precursor protein and phospholipase D1. J. Biol. Chem. 284: 12145–12152. https://doi.org/10.1074/jbc.M808497200

Liu, Z., T. Zhou, A. C. Ziegler, P. Dimitrion, and L. Zuo, 2017 Oxidative stress in neurodegenerative diseases: from molecular mechanisms to clinical applications. Oxid. Med. Cell. Longev. 2017: 2525967. https://doi.org/10.1155/2017/2525967

Mackenzie, I. R., R. Rademakers, and M. Neumann, 2010 TDP-43 and FUS in amyotrophic lateral sclerosis and frontotemporal dementia. Lancet Neurol. 9: 995–1007. https://doi.org/10.1016/S1474-4422(10)70195-2

Markmiller, S., S. Soltanieh, K. L. Server, R. Mak, W. Jin *et al.*, 2018 Context-dependent and disease-specific diversity in protein interactions within stress granules. Cell 172: 590–604.e13. https://doi.org/10.1016/j.cell.2017.12.032

Maruyama, H., H. Morino, H. Ito, Y. Izumi, H. Kato *et al.*, 2010 Mutations of optineurin in amyotrophic lateral sclerosis. Nature 465: 223–226. https://doi.org/10.1038/nature08971

McGurk, L., A. Berson, and N. M. Bonini, 2015 Drosophila as an in vivo model for human neurodegenerative disease. Genetics 201: 377–402. https://doi.org/10.1534/genetics.115.179457

Michlewski, G., J. R. Sanford, and J. F. Caceres, 2008 The splicing factor SF2/ASF regulates translation initiation by enhancing phosphorylation of 4E–BP1. Mol. Cell 30: 179–189. https://doi.org/10.1016/j.molcel.2008.03.013

Miguel, L., T. Frebourg, D. Campion, and M. Lecourtois, 2011 Both cytoplasmic and nuclear accumulations of the protein are neurotoxic in Drosophila models of TDP-43 proteinopathies. Neurobiol. Dis. 41: 398–406. https://doi.org/10.1016/j.nbd.2010.10.007

Mi, H., A. Muruganujan, J. T. Casagrande, and P. D. Thomas, 2013 Large-scale gene function analysis with the PANTHER

classification system. Nat. Protoc. 8: 1551–1566. https://doi.org/10.1038/nprot.2013.092

Moreira, M. C., S. Klur, M. Watanabe, A. H. Nemeth, I. Le Ber *et al.*, 2004 Senataxin, the ortholog of a yeast RNA helicase, is mutant in ataxia-ocular apraxia 2. Nat. Genet. 36: 225–227. https://doi.org/10.1038/ng1303

Moujalled, D., and A. R. White, 2016 Advances in the development of disease-modifying treatments for amyotrophic lateral sclerosis. CNS Drugs 30: 227–243. https://doi.org/10.1007/s40263-016-0317-8

Nagy, M., W. A. Fenton, D. Li, K. Furtak, and A. L. Horwich, 2016 Extended survival of misfolded G85R SOD1-linked ALS mice by transgenic expression of chaperone Hsp110. Proc. Natl. Acad. Sci. USA 113: 5424–5428. https://doi.org/10.1073/pnas.1604885113

Neumann, M., D. M. Sampathu, L. K. Kwong, A. C. Truax, M. C. Micsenyi *et al.*, 2006 Ubiquitinated TDP-43 in frontotemporal lobar degeneration and amyotrophic lateral sclerosis. Science 314: 130–133. https://doi.org/10.1126/science.1134108

Pallavi, S. K., D. M. Ho, C. Hicks, L. Miele, and S. Artavanis-Tsakonas, 2012 Notch and Mef2 synergize to promote proliferation and metastasis through JNK signal activation in Drosophila. EMBO J. 31: 2895–2907. https://doi.org/10.1038/emboj.2012.129

Parks, A. L., K. R. Cook, M. Belvin, N. A. Dompe, R. Fawcett *et al.*, 2004 Systematic generation of high-resolution deletion coverage of the Drosophila melanogaster genome. Nat. Genet. 36: 288–292. https://doi.org/10.1038/ng1312

Peng, X., and M. A. Frohman, 2012 Mammalian phospholipase D physiological and pathological roles. Acta Physiol. (Oxf.) 204: 219–226. https://doi.org/10.1111/j.1748-1716.2011.02298.x

Periz, G., J. Lu, T. Zhang, M. W. Kankel, A. M. Jablonski *et al.*, 2015 Regulation of protein quality control by UBE4B and LSD1 through p53-mediated transcription. PLoS Biol. 13: e1002114. https://doi.org/10.1371/journal.pbio.1002114

Prasad, D. D., M. Ouchida, L. Lee, V. N. Rao, and E. S. Reddy, 1994 TLS/FUS fusion domain of TLS/FUS-erg chimeric protein resulting from the t(16;21) chromosomal translocation in human myeloid leukemia functions as a transcriptional activation domain. Oncogene 9: 3717–3729.

Rabin, S. J., J. M. Kim, M. Baughn, R. T. Libby, Y. J. Kim *et al.*, 2010 Sporadic ALS has compartment-specific aberrant exon splicing and altered cell-matrix adhesion biology. Hum. Mol. Genet. 19: 313–328. https://doi.org/10.1093/hmg/ddp498

Raghu, P., E. Coessens, M. Manifava, P. Georgiev, T. Pettitt *et al.*, 2009 Rhabdomere biogenesis in Drosophila photoreceptors is acutely sensitive to phosphatidic acid levels. J. Cell Biol. 185: 129–145. https://doi.org/10.1083/jcb.200807027

Ramaswami, M., J. P. Taylor, and R. Parker, 2013 Altered ribostasis: RNA-protein granules in degenerative disorders. Cell 154: 727–736. https://doi.org/10.1016/j.cell.2013.07.038

Rao, S., M. Lam, Y. Wing, L. Yim, W. Chu *et al.*, 2015 Beneficial effect of phosphatidylcholine supplementation in alleviation of hypomania and insomnia in a Chinese bipolar hypomanic boy and a possible explanation to the effect at the genetic level. Springerplus 4: 235. https://doi.org/10.1186/s40064-015-1002-y

Renton, A. E., E. Majounie, A. Waite, J. Simon-Sanchez, S. Rollinson *et al.*, 2011 A hexanucleotide repeat expansion in C9ORF72 is the cause of chromosome 9p21-linked ALS-FTD. Neuron 72: 257–268. https://doi.org/10.1016/j.neuron.2011.09.010

Renton, A. E., A. Chio, and B. J. Traynor, 2014 State of play in amyotrophic lateral sclerosis genetics. Nat. Neurosci. 17: 17–23. https://doi.org/10.1038/nn.3584

Rickman, O. J., E. L. Baple, and A. H. Crosby, 2019 Lipid metabolic pathways converge in motor neuron degenerative diseases. Brain 143: 1073–1087. https://doi.org/10.1093/brain/awz382

Ritson, G. P., S. K. Custer, B. D. Freibaum, J. B. Guinto, D. Geffel *et al.*, 2010 TDP-43 mediates degeneration in a novel Drosophila model of disease caused by mutations in VCP/p97. J. Neurosci. 30: 7729–7739. https://doi.org/10.1523/JNEUROSCI.5894-09.2010

Ross, C. A., and M. A. Poirier, 2004 Protein aggregation and neurodegenerative disease. Nat. Med. 10: S10–S17. https://doi.org/10.1038/nm1066

Rothstein, J. D., 2009 Current hypotheses for the underlying biology of amyotrophic lateral sclerosis. Ann. Neurol. 65: S3–S9. https://doi.org/10.1002/ana.21543

Rowland, L. P., 2001 How amyotrophic lateral sclerosis got its name the clinical-pathologic genius of Jean-Martin Charcot. Arch. Neurol. 58: 512–515.

Sanematsu, F., A. Nishikimi, M. Watanabe, T. Hongu, Y. Tanaka *et al.*, 2013 Phosphatidic acid-dependent recruitment and function of the Rac activator DOCK1 during dorsal ruffle formation. J. Biol. Chem. 288: 8092–8100. https://doi.org/10.1074/jbc.M112.410423

Sanford, J. R., N. K. Gray, K. Beckmann, and J. F. Caceres, 2004 A novel role for shuttling SR proteins in mRNA translation. Genes Dev. 18: 755–768. https://doi.org/10.1101/gad.286404

Sato, T., T. Hongu, M. Sakamoto, Y. Funakoshi, and Y. Kanaho, 2013 Molecular mechanisms of N-formyl-methionyl-leucyl-phenylalanine-induced superoxide generation and degranulation in mouse neutrophils: phospholipase D is dispensable. Mol. Cell. Biol. 33: 136–145. https://doi.org/10.1128/MCB.00869-12

Sen, A., D. N. Dimlich, K. G. Guruharsha, M. W. Kankel, K. Hori *et al.*, 2013 Genetic circuitry of Survival motor neuron, the gene underlying spinal muscular atrophy. Proc. Natl. Acad. Sci. USA 110: E2371–E2380. https://doi.org/10.1073/pnas.1301738110

Song, Y., M. Nagy, W. Nic, N. K. Tyagi, W. A. Fenton *et al.*, 2013 Molecular chaperone Hsp110 rescues a vesicle transport defect produced by an ALS-associated mutant SOD1 protein in squid axoplasm. Proc. Natl. Acad. Sci. USA 110: 5428–5433. https://doi.org/10.1073/pnas.1303279110

Staats, K. A., L. Van Helleputte, A. R. Jones, A. Bento-Abreu, A. Van Hoecke *et al.*, 2013 Genetic ablation of phospholipase C delta 1 increases survival in SOD1(G93A) mice. Neurobiol. Dis. 60: 11–17. https://doi.org/10.1016/j.nbd.2013.08.006

Stegner, D., I. Thielmann, P. Kraft, M. A. Frohman, G. Stoll *et al.*, 2013 Pharmacological inhibition of phospholipase D protects mice from occlusive thrombus formation and ischemic stroke–brief report. Arterioscler. Thromb. Vasc. Biol. 33: 2212–2217. https://doi.org/10.1161/ATVBAHA.113.302030

Su, W., O. Yeku, S. Olepu, A. Genna, J. S. Park *et al.*, 2009 5-Fluoro-2-indolyl des-chlorohalopemide (FIPI), a phospholipase D pharmacological inhibitor that alters cell spreading and inhibits chemotaxis. Mol. Pharmacol. 75: 437–446. https://doi.org/10.1124/mol.108.053298

Sun, Z., Z. Diaz, X. Fang, M. P. Hart, A. Chesi *et al.*, 2011 Molecular determinants and genetic modifiers of aggregation and toxicity for the ALS disease protein FUS/TLS. PLoS Biol. 9: e1000614. https://doi.org/10.1371/journal.pbio.1000614

Sung, J. Y., S. Y. Lee, D. S. Min, T. Y. Eom, Y. S. Ahn *et al.*, 2001 Differential activation of phospholipases by mitogenic EGF and neurogenic PDGF in immortalized hippocampal stem cell lines. J. Neurochem. 78: 1044–1053. https://doi.org/10.1046/j.1471-4159.2001.00491.x

Taes, I., M. Timmers, N. Hersmus, A. Bento-Abreu, L. Van Den Bosch *et al.*, 2013 Hdac6 deletion delays disease progression in the SOD1G93A mouse model of ALS. Hum. Mol. Genet. 22: 1783–1790. https://doi.org/10.1093/hmg/ddt028

Tan, A. Y., and J. L. Manley, 2009 The TET family of proteins: functions and roles in disease. J. Mol. Cell Biol. 1: 82–92. https://doi.org/10.1093/jmcb/mjp025

Tanishima, M., S. Takashima, A. Honda, D. Yasuda, T. Tanikawa *et al.*, 2017 Identification of optineurin as an Interleukin-1 receptor-associated kinase 1-binding protein and its role in regulation of MyD88-dependent signaling. J Biol Chem. 292: 17250–17257. https://doi.org/10.1074/jbc.M117.813899

Tateishi, T., T. Hokonohara, R. Yamasaki, S. Miura, H. Kikuchi *et al.*, 2010 Multiple system degeneration with basophilic inclusions in Japanese ALS patients with FUS mutation. Acta Neuropathol. 119: 355–364. https://doi.org/10.1007/s00401-009-0621-1

Thibault, S. T., M. A. Singer, W. Y. Miyazaki, B. Milash, N. A. Dompe *et al.*, 2004 A complementary transposon tool kit for Drosophila melanogaster using P and piggyBac. Nat. Genet. 36: 283–287. https://doi.org/10.1038/ng1314

Turner, M. R., O. Hardiman, M. Benatar, B. R. Brooks, A. Chio *et al.*, 2013 Controversies and priorities in amyotrophic lateral sclerosis. Lancet Neurol. 12: 310–322. https://doi.org/10.1016/S1474-4422(13)70036-X

Vance, C., B. Rogelj, T. Hortobágyi, K. J. De Vos, A. L. Nishimura *et al.*, 2009 Mutations in FUS, an RNA processing protein, cause familial amyotrophic lateral sclerosis type 6. Science 323: 1208–1211. https://doi.org/10.1126/science.1165942

Voigt, A., D. Herholz, F. C. Fiesel, K. Kaur, D. Muller *et al.*, 2010 TDP-43-mediated neuron loss in vivo requires RNA-binding activity. PLoS One 5: e12247. https://doi.org/10.1371/journal.pone.0012247

Wang, J. W., J. R. Brent, A. Tomlinson, N. A. Shneider, and B. D. McCabe, 2011 The ALS-associated proteins FUS and TDP-43 function together to affect Drosophila locomotion and life span. J. Clin. Invest. 121: 4118–4126. https://doi.org/10.1172/JCI57883

Wegorzewska, I., S. Bella, N. J. Cairnsa, T. M. Millera, and R. H. Baloh, 2009 TDP-43 mutant transgenic mice develop features of ALS and frontotemporal lobar degeneration. Proc. Natl. Acad. Sci. USA 106: 18809–18814. https://doi.org/10.1073/pnas.0908767106

Winton, M. J., L. M. Igaz, M. M. Wong, L. K. Kwong, J. Q. Trojanowski *et al.*, 2008 Disturbance of nuclear and cytoplasmic TAR DNA-binding protein (TDP-43) induces disease-like redistribution, sequestration, and aggregate formation. J. Biol. Chem. 283: 13302–13309. https://doi.org/10.1074/jbc.M800342200

Xia, R., Y. Liu, L. Yang, J. Gal, H. Zhu *et al.*, 2012 Motor neuron apoptosis and neuromuscular junction perturbation are prominent features in a Drosophila model of Fus-mediated ALS. Mol. Neurodegener. 7: 10. https://doi.org/10.1186/1750-1326-7-10

Xu, Y. F., T. F. Gendron, Y. J. Zhang, W. L. Lin, S. D'Alton *et al.*, 2010 Wild-type human TDP-43 expression causes TDP-43 phosphorylation, mitochondrial aggregation, motor deficits, and early mortality in transgenic mice. J. Neurosci. 30: 10851–10859. https://doi.org/10.1523/JNEUROSCI.1630-10.2010

Xu, Z., M. Poidevin, X. Li, Y. Li, L. Shu *et al.*, 2013 Expanded GGGGCC repeat RNA associated with amyotrophic lateral sclerosis and frontotemporal dementia causes neurodegeneration. Proc. Natl. Acad. Sci. USA 110: 7778–7783. https://doi.org/10.1073/pnas.1219643110

Yoon, M. S., C. Yon, S. Y. Park, D. Y. Oh, A. H. Han *et al.*, 2005 Role of phospholipase D1 in neurite outgrowth of neural stem cells. Biochem. Biophys. Res. Commun. 329: 804–811. https://doi.org/10.1016/j.bbrc.2005.02.087

Yu, C., K. H. Wan, A. S. Hammonds, M. Stapleton, J. W. Carlson *et al.*, 2011 Development of expression-ready constructs for generation of proteomic libraries. Methods Mol. Biol. 723: 257–272. https://doi.org/10.1007/978-1-61779-043-0_17

Yuva-Aydemir, Y., S. Almeida, G. Krishnan, T. F. Gendron, and F. B. Gao, 2019 Transcription elongation factor AFF2/FMR2 regulates expression of expanded GGGGCC repeat-containing C9ORF72 allele in ALS/FTD. Nat. Commun. 10: 5466. https://doi.org/10.1038/s41467-019-13477-8

Zhang, Z., and A. R. Krainer, 2004 Involvement of SR proteins in mRNA surveillance. Mol. Cell 16: 597–607. https://doi.org/10.1016/j.molcel.2004.10.031

Zhang, Y., and M. A. Frohman, 2014 Cellular and physiological roles for phospholipase D1 in cancer. J. Biol. Chem. 289: 22567–22574. https://doi.org/10.1074/jbc.R114.576876

Zhang, Y., S. Kwon, T. Yamaguchi, F. Cubizolles, S. Rousseaux *et al.*, 2008 Mice lacking histone deacetylase 6 have hyperacetylated tubulin but are viable and develop normally. Mol. Cell. Biol. 28: 1688–1701. https://doi.org/10.1128/MCB.01154-06

Zhang, S., R. Binari, R. Zhou, and N. Perrimon, 2010 A genome-wide RNA interference screen for modifiers of aggregates formation by mutant Huntingtin in Drosophila. Genetics 184: 1165–1179. https://doi.org/10.1534/genetics.109.112516

Zhang, K., C. J. Donnelly, A. R. Haeusler, J. C. Grima, J. B. Machamer *et al.*, 2015 The C9orf72 repeat expansion disrupts nucleocytoplasmic transport. Nature 525: 56–61. https://doi.org/10.1038/nature14973

Zhu, Y. B., K. Kang, Y. Zhang, C. Qi, G. Li *et al.*, 2012 PLD1 negatively regulates dendritic branching. J. Neurosci. 32: 7960–7969. https://doi.org/10.1523/JNEUROSCI.5378-11.2012

Zuo, P., and J. L. Manley, 1993 Functional domains of the human splicing factor ASF/SF2. EMBO J. 12: 4727–4737. https://doi.org/10.1002/j.1460-2075.1993.tb06161.x

Communicating editor: H. Bellen